27. *Seismic Waves due to Tractions Applied to the Inner Surface of a Spherical Cavity in an Elastic Earth.*

By Genrokuro NISHIMURA and Takeo TAKAYAMA,

Earthquake Research Institute.

(Received March 20, 1938.)

1. In the present paper, which is a continuation of the previous one[1], we shall, with the aid of numerous figures, deal with wave-phenomena in the following two cases; [1] that in which the inner surface of a spherical cavity in an elastic earth is subjected to normal traction of shock type, [2] that in which the inner surface of the cavity is subjected to a shearing force of the same type.

2. Now let the boundary-conditions on the inner surface of a spherical cavity in an elastic earth be expressed as follows[2]:

When $t \geqq 0$,

$$\widehat{rr}_{r=a} = -P\frac{t}{t_m}\exp\{1-t/t_m\}, \quad \widehat{r\theta}_{r=a} = \widehat{r\phi}_{r=a} = 0,$$

and when $t \leqq 0$,

$$\widehat{rr}_{r=a} = \widehat{r\theta}_{r=a} = \widehat{r\phi}_{r=a} = 0. \qquad (1)$$

Then the radial vibrations of a particle in the earth due to the longitudinal wave that issues from the cavity are expressed by

$$u = \frac{aP}{\mu}\left(\frac{a}{r}\right)\left[\frac{\alpha(V/v)^3}{\sqrt{1-(V/v)^2}}\frac{\{4\alpha-4(V/v)^2-\alpha^2\}}{\{4(V/v)^2-4(V/v)^2\alpha+\alpha^2\}^2}\cdot\right.$$
$$\cdot\exp\{1-2(V/v)^2\tau\}\cdot\sin\left\{2(V/v)\sqrt{1-(V/v)^2}\tau\right\}$$
$$+\frac{\alpha(V/v)^2\{\alpha^2-4(V/v)^2\}}{\{4(V/v)^2-4(V/v)^2\alpha+\alpha^2\}^2}\exp\{1-2(V/v)^2\tau\}\cdot$$
$$\left.\cdot\cos\left\{2(V/v)\sqrt{1-(V/v)^2}\tau\right\}\right.$$

1) G. NISHIMURA, *Bull. Earthq. Res. Inst.*, **15** (1937), 614~635.

2) The meanigs of the notations used in the present paper are explained in the previous paper. G. NISHIMURA, *loc. cit.*

$$+\frac{\alpha(V/v)^2\{4(V/v)^2-\alpha^2\}}{\{4(V/v)^2-4(V/v)^2\alpha+\alpha^2\}^2}\exp\{1-\alpha\tau\}$$

$$-\frac{\alpha^2(V/v)^2}{\{4(V/v)^2-4(V/v)^2\alpha+\alpha^2\}}\tau\exp\{1-\alpha\tau\}\Bigg]$$

$$+\frac{aP}{\mu}\left(\frac{a}{r}\right)^2\Bigg[\frac{\alpha(V/v)}{2\sqrt{1-(V/v)^2}}\frac{\{\alpha^2-4(V/v)^2\alpha-4(V/v)^2\}+8(V/v)^4}{\{4(V/v)^2-4(V/v)^2\alpha+\alpha^2\}^2}\cdot$$

$$\cdot\exp\{1-2(V/v)^2\tau\}\sin\left\{2(V/v)\sqrt{1-(V/v)^2}\tau\right\}$$

$$+\frac{2(V/v)^2\alpha\{2(V/v)^2-\alpha\}}{\{4(V/v)^2-4(V/v)^2\alpha+\alpha^2\}^2}\exp\{1-2(V/v)^2\tau\}\cdot$$

$$\cdot\cos\left\{2(V/v)\sqrt{1-(V/v)^2}\tau\right\}$$

$$+\frac{2(V/v)^2\alpha\{\alpha-2(V/v)^2\}}{\{4(V/v)^2-4(V/v)^2\alpha+\alpha^2\}^2}\exp\{1-\alpha\tau\}$$

$$+\frac{\alpha(V/v)^2}{\{4(V/v)^2-4(V/v)^2\alpha+\alpha^2\}}\tau\exp\{1-\alpha\tau\}\Bigg], \qquad (2)$$

where

$$\alpha=\frac{a}{t_m v},\quad \tau=\frac{v}{a}\left(t-\frac{r-a}{v}\right),\quad v=\sqrt{\frac{\lambda+2\mu}{\rho}},\quad V=\sqrt{\frac{\mu}{\rho}}. \qquad (3)$$

Expression (2) may easily be deduced from expression (12) of the previous paper[3]. It may be seen from expression (2) that the longitudinal waves generated by a normal (perpendicular) force of shock type (1) are of three kinds; [1] waves of the same time-variation as the force applied to the cavity, [2] waves of sinusoidal time-variation, and [3] other waves with an aperiodic damping time-variation that are set up in order to satisfy the initial conditions on the boundary of the cavity. For ease of reference, we shall refer to the first, second, and third kinds of waves as FORCED, FREE[4] and COMPLEMENTARY WAVES. In other words,

$$\text{the waves that emanate from the cavity} = \text{the forced waves} + \text{the free waves} + \text{the complementary waves}. \qquad (4)$$

3) G. NISHIMURA, *loc. cit.*

4) Naturally, both the periods and the damping ratio of the free waves, which are respectively expressed by $\frac{\pi}{(V/v)\sqrt{1-(V/v)^2}}\frac{a}{v}$, $e^{\pi\frac{(V/v)}{\sqrt{1-(V/v)^2}}}$ in the present case, do not depend on the mode of time-variation in the stress applied to the inner surface of the cavity, although their intensities depend entirely on it. H. KAWASUMI and R. YOSHIYAMA. *Disin*, 7 (1935), 367.

The respective amplitudes of these three kinds of waves are functions of the value of $a/(t_m v)$, which we may call the rapidity of the stress applied to the cavity. We notice from expression (2) that when $a/(t_m v) \to 0$, only the following forced waves issue from the cavity:

$$u = \frac{1}{4}\frac{aP}{\mu}\left(\frac{a}{r}\right)^2 \frac{1}{t_m}\left(t - \frac{r-a}{v}\right)\exp\left\{1 - \frac{1}{t_m}\left(t - \frac{r-a}{v}\right)\right\},$$

of which the amplitudes are proportional to the square of the inverse ratio of the distance from the centre of the cavity—a fact which shows that the wave-phenomena occur when $a/(t_m v) \to 0$, is likely to be the same as in the statical problem.

Since the damping ratio σ_f[5] of the free wave is give by $e^{\pi\sqrt{1-2\sigma}}$, when Poisson's ratio becomes 0·50, σ_f becomes unity. If therefore, we hypothetically suppose that the value of the Poisson ratio of the material changes temporally from the normal value[6] to a value near 0·50 on and near the earthquake origin only at the instant the seismic waves emanate from the origin, it will be seen that even if one shock were applied to the earthquake origin, the seismic waves emanating from that origin would consist of many regular trains of oscillatory waves, the damping ratio of which is nearly unity.

To get the nature of the wave-motion of particles that are some distance away from the cavity, we obtain from expression (2) the following approximate expression for longitudinal waves:

$$u_{r\to\infty} \simeq u_{\text{free}} + u_{\text{forced}} + u_{\text{complementary}}, \tag{5}$$

where u_{free}, u_{forced}, and $u_{\text{complementary}}$ are respectively the free, forced, and complementary waves that emanate from the cavity, and which are expressed by

$$u_{\text{free}} = \frac{aP}{\mu}\left(\frac{a}{r}\right)\left[\frac{\alpha(V/v)^3}{\sqrt{1-(V/v)^2}}\cdot\right.$$

$$\cdot\frac{\{4\alpha - 4(V/v)^2 - \alpha^2\}}{\{4(V/v)^2 - 4(V/v)^2\alpha + \alpha^2\}^2}\exp\{1 - 2(V/v)^2\tau\}\cdot$$

$$\left.\cdot\sin\left\{2(V/v)\sqrt{1-(V/v)^2}\tau\right\}\right.$$

5) See foot note 4).

6) In the earth's cruts, the normal value of Poisson's ratio is assumed to be nearly 0·25.

$$+\frac{\alpha(V/v)^2\{\alpha^2-4(V/v)^2\}}{\{4(V/v)^2-4(V/v)^2\alpha+\alpha^2\}^2}\exp\{1-2(V/v)^2\tau\}\cdot$$

$$\cdot\cos\left\{2(V/v)\sqrt{1-(V/v)^2}\tau\right\}\Bigg], \qquad \text{(a)}$$

$$u_{\text{forced}}=-\frac{aP}{\mu}\left(\frac{a}{r}\right)\frac{\alpha^2(V/v)^2}{\{4(V/v)^2-4(V/v)^2\alpha+\alpha^2\}}\tau\exp\{1-\alpha\tau\}, \qquad \text{(b)} \qquad (6)$$

$$u_{\text{complementary}}=\frac{aP}{\mu}\left(\frac{a}{r}\right)\frac{\alpha(V/v)^2\{4(V/v)^2-\alpha^2\}}{\{4(V/v)^2-4(V/v)^2\alpha+\alpha^2\}^2}\exp\{1-\alpha\tau\}\cdot \qquad \text{(c)}$$

From expression (5), we obtain Figs. 1~12, in which are shown the radial vibrations of particles for various values of $a/(t_m v)$ in the elastic earth, the Poisson ratio of which is 1/4. From Figs. 1~12, we see that when rapidity $a/(t_m v)$ becomes large, the oscillatory nature of the wave-motion of the particle increases, and it will be seen, besides, that both the amplitudes and the apparent periods in a state of initial motion, as well as the apparent damping ratios of the radial vibrations of par-

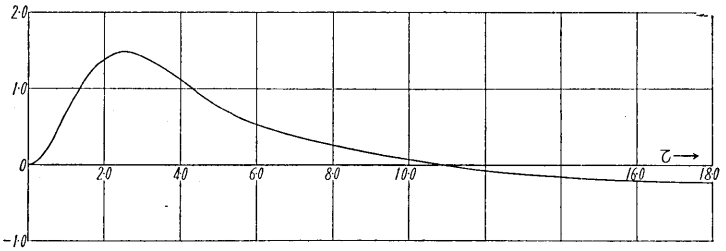

Fig. 1. $\frac{a}{t_m v}=0{\cdot}10$. The unit of the vertical scale$=\frac{u_{r\to\infty}}{aP/\mu\cdot(a/r)}$.

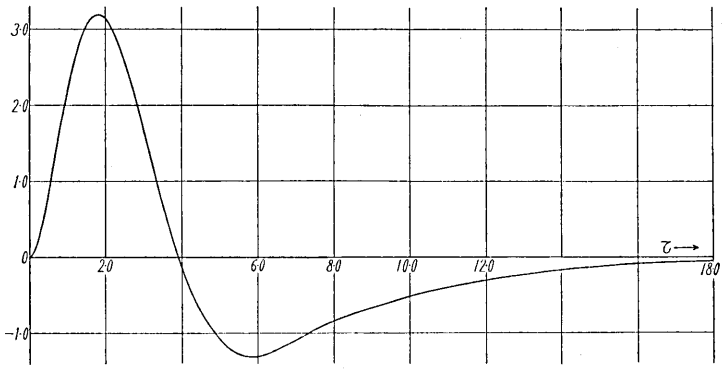

Fig. 2. $\frac{a}{t_m v}=0{\cdot}4$. The unit of the vertical scale$=\frac{u_{r\to\infty}}{aP/\mu\cdot(a/r)}$.

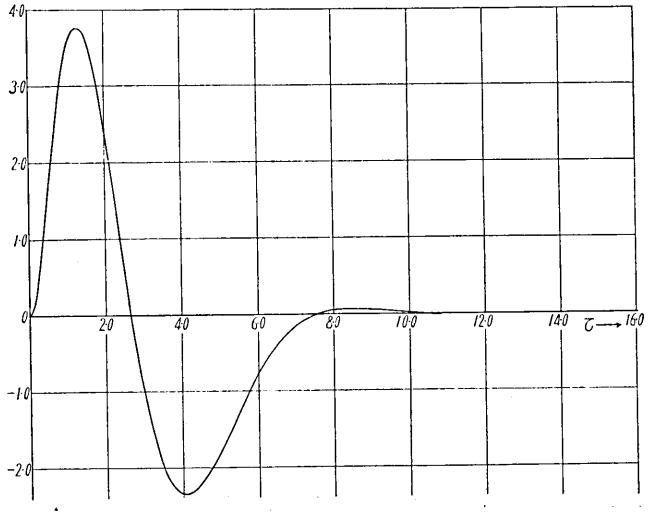

Fig. 3. $\frac{a}{t_m v}=1{\cdot}0$. The unit of the vertical scale$=\frac{u_{r\to\infty}}{aP/\mu\cdot(a/r)}$.

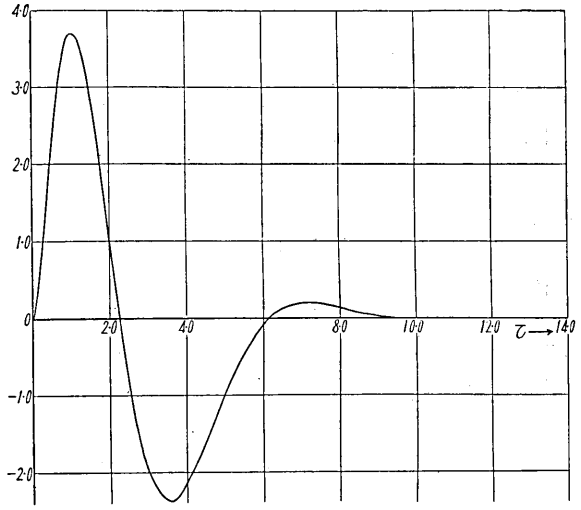

Fig. 4. $\frac{a}{t_m v}=1{\cdot}5$. The unit of the vertical scale$=\frac{u_{r\to\infty}}{aP/\mu\cdot(a/r)}$.

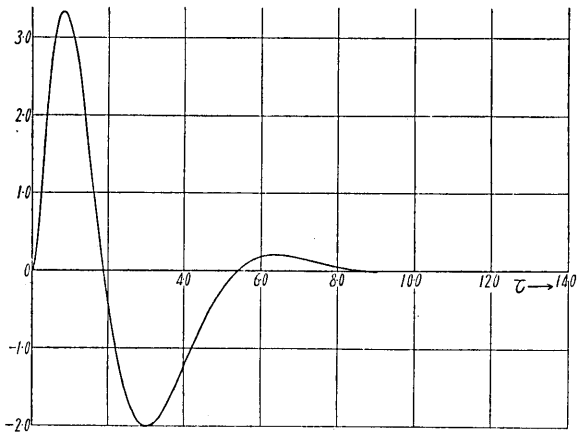

Fig. 5. $\frac{a}{t_m v}=2\cdot0$. The unit of the vertical scale$=\frac{u_{r\to\infty}}{aP/\mu\cdot(a/r)}$.

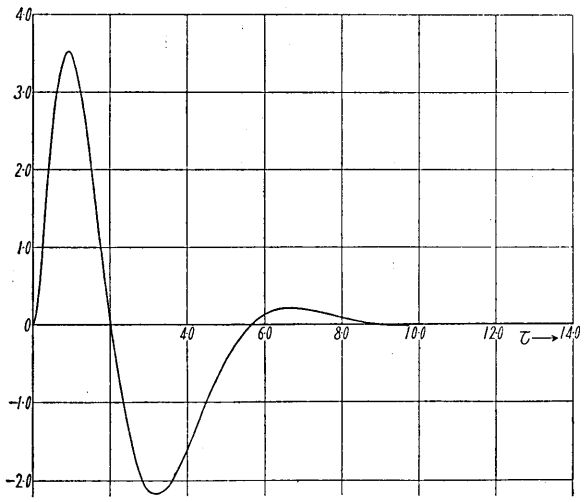

Fig. 6. $\frac{a}{t_m v}=2\cdot4$. The unit of the vertical scale$=\frac{u_{r\to\infty}}{aP/\mu\cdot(a/r)}$.

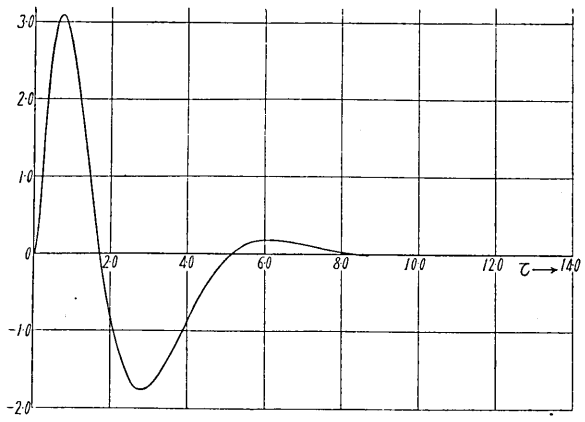

Fig. 7. $\frac{a}{t_m v}=3\cdot0$. The nnit of the vertical scale$=\frac{u_{r\to\infty}}{aP/\mu\cdot(a/r)}$.

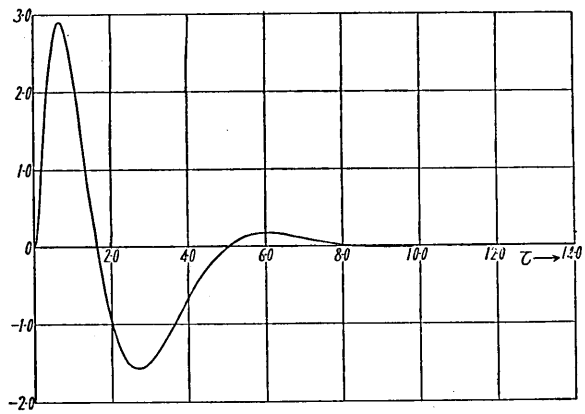

Fig. 8. $\frac{a}{t_m v}=3\cdot5$. The unit of the vertical scale$=\frac{u_{r\to\infty}}{aP/\mu\cdot(a/r)}$.

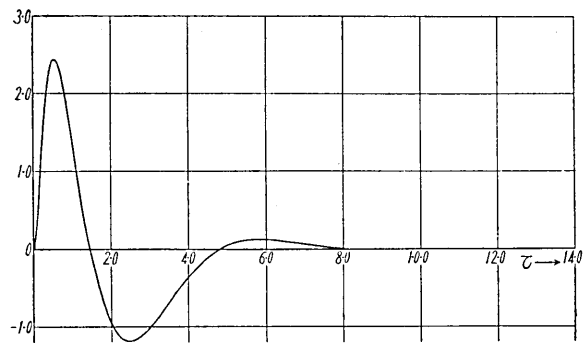

Fig. 9. $\frac{a}{t_m v}=5\cdot0$. The unit of the vertical scale$=\frac{u_{r\to\infty}}{aP/\mu\cdot(a/r)}$.

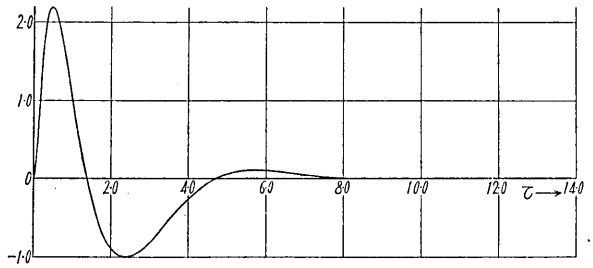

Fig. 10. $\frac{a}{t_m v}=6{\cdot}0$. The unit of the vertical scale$=\frac{u_{r\to\infty}}{aP/\mu\cdot(a/r)}$.

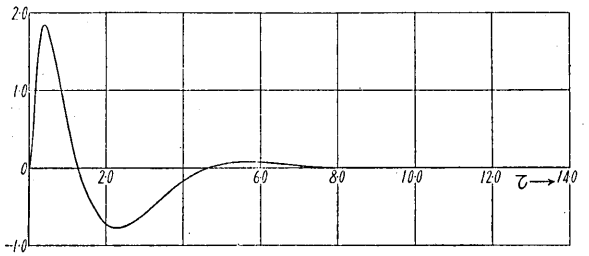

Fig. 11. $\frac{a}{t_m v}=8{\cdot}0$. The unit of the vertical scale$=\frac{u_{r\to\infty}}{aP/\mu\cdot(a/r)}$.

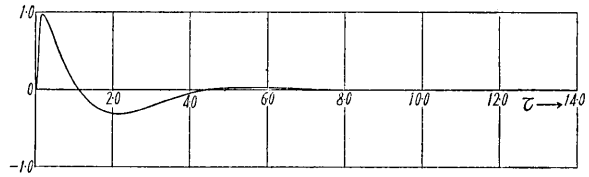

Fig. 12. $\frac{a}{t_m v}=20{\cdot}0$. The unit of the vertical scale$=\frac{U_{r\to\infty}}{aP/\mu\cdot(a/r)}$.

ticles, vary entirely with the rapidity of the stress applied to the cavity. Using Figs. 1~12, we obtain Figs. 13, 14, which respectively show the amplitudes and the apparent periods of the radial vibrations in a state of

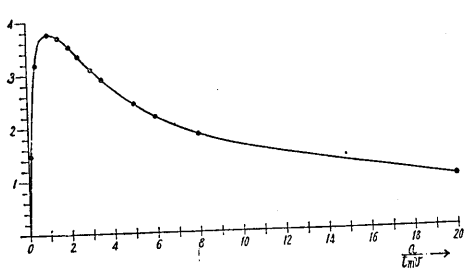

Fig. 13.

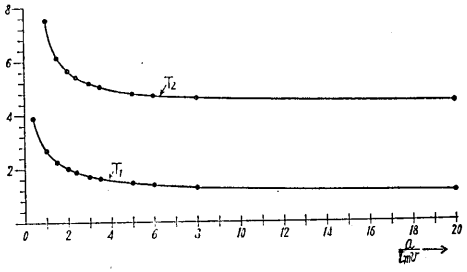

Fig. 14.

initial motion, the abscissae in these Figs. being the value of $a/(t_m v)$.

It will be seen from Fig. 13 that the amplitude of initial motion of a particle due to the longitudinal wave becomes maximum when $a/(t_m v) \fallingdotseq 1$, and also that when $a/(t_m v)$ becomes nil or increases infinitely, it becomes nil or very small respectively. It is not easy to understand the reason for the maximum amplitude of the initial wave-motion's occurring when $a/(t_m v) \fallingdotseq 1$, although the reason for the spectrum-like nature of the amplitude of wave-motion, as shown in Fig. 13, will be understood by calculating the kinetic energy as the result of the applied stress on the inner surface of the cavity. A spectrum-like nature of vibration-amplitude in a state of initial motion, as shown in Fig. 13, is also conceived for the case of a steady state[7], in which an infinite train of harmonic forced waves emanates from a spherical cavity as the result of the normal pressure of simple-harmonic time-variations applied to its inner surface, although such free and complementary waves as mentioned in the present paper do not actually issue from it.

Curves T_1 and T_2 in Fig. 14, which are obtained by using Figs. 1~12, show respectively the duration of time from the beginning of vibration to the time when the displacement-amplitude first becomes nil, and those from the beginning of the motion to the time when the displacement becomes nil for the second time. For ease of reference, we shall refer to the former duration of time as the apparent half-period and the latter as the apparent period of vibration in a state of initial motion.

It will be seen from Fig. 14 that the greater the rapidity of the pressure applied to the cavity, the shorter the apparent period of radial vibration in a state of initial motion. As in the case of an infinite train of forced waves emanating from the cavity owing to the pressure of simple-harmonic time-variation applied to its inner surface, the apparent period of the forced wave contained in expression (6)b is the linear function of the rapidity of the applied pressure. The fact that the relation between the apparent period of the initial motion and the rapidity of thc applied pressure, as will be seen from Fig. 14, is not

---

7) When $\widehat{rr}_{r=a} = -Pe^{i\frac{2\pi}{T}}$ and $\widehat{r\theta}_{r=a} = \widehat{r\phi} = 0$, the radial vibrations of particles that are some distance away from the cavity and which are due to the longitudinal forced waves issuing from it, are expressed by

$$u_{r\to\infty} \fallingdotseq \frac{Pa}{\mu}\left(\frac{a}{r}\right)\frac{\sqrt{16\alpha^4+4\alpha^2\{1-\alpha^2(v/V)^2\}^2}}{4[4\alpha^2+\{1-\alpha^2(v/V)^2\}^2]}\, e^{i\left\{2\pi\left(\frac{t}{T}-\frac{r-a}{L}\right)+\tan^{-1}\zeta\right\}},$$

where $\alpha = \pi\frac{a}{L}$, $\zeta = (2\alpha)/\{1-\alpha^2(v/V)^2\}$, L=the wave-length of the forced wave. From this expression, it will be seen that the amplitude becomes maximum when $L/a = 1{\cdot}0$, and that the vibration-amplitudes of the particles exhibit a spectrum-like nature with variations in the value of L/a.

so simple as in the case of the forced wave, is mainly owing to the existence of both free and complementary waves in addition to the forced wave. As will be seen from Fig. 14, even if should rapidity of the applied pressure become very pronounced, the apparent period of the initial motion does not become so markedly small.

3. The wave-motions of particles that lie some distance away from a spherical cavity in an elastic earth have already been discussed for the case when the normal stress $\widehat{rr}$ on the inner surface of the cavity has co-latitudinal and azimuthal distributions, like $\widehat{rr}_{r=a}=-f(t)\sin 2\theta\cdot\cos\phi$, and the shearing stresses on this surface ($\widehat{r\theta}_{r=a}$, $\widehat{r\phi}_{r=a}$) are zero. Now let the time-factor $f(t)$ in expressions[8] (26)$\sim$(32), which are obtained in the case when Poisson's ratio $=1/4$, in the previous paper, be as follows:

$$\left.\begin{array}{lll} \text{When} & t\geqq 0, & f(t)=t/t_m\cdot\exp\{1-t/t_m\}\,, \\ \text{and when} & t\leqq 0, & f(t)=0, \end{array}\right\} \tag{7}$$

as in Art. 2. Then the radial, co-latitudinal and azimuthal components of displacement u_1, v_3, w_3, which are some distance away from the cavity, are expressed by

$$\left.\begin{aligned} u_1 &\approx -\frac{1}{6\pi}\frac{V^2vP}{\mu a^3}\frac{1}{r}\sin 2\theta\cos\cdot X\Big(t-\frac{1}{v}(r-a)\Big), && \text{(a)} \\ v_3 &\approx \frac{1}{3\pi}\frac{v^4P}{\mu V a^3}\frac{1}{r}\cos 2\theta\cos\theta\cdot Y\Big(t-\frac{1}{V}(r-a)\Big), && \text{(b)} \\ w_3 &\approx -\frac{1}{3\pi}\frac{v^4P}{\mu V a^3}\frac{1}{r}\cos\theta\sin\phi\cdot Y\Big(t-\frac{1}{V}(r-a)\Big), && \text{(c)} \end{aligned}\right\} \tag{8}$$

where

$$X\Big(t-\frac{1}{v}(r-a)\Big)=\frac{1}{t_m}\int_{-\infty}^{\infty}\frac{P'(p)}{\psi'(p)}\frac{e^{1-tp\left\{t-\frac{1}{v}(r-a)\right\}}}{\Big(p-i\frac{1}{t_m}\Big)^2}dp, \tag{9}$$

$$Y\Big(t-\frac{1}{V}(r-a)\Big)=\frac{1}{t_m}\int_{-\infty}^{\infty}\frac{T'(p)}{\psi'(p)}\frac{e^{1-tp\left\{t-\frac{1}{V}(r-a)\right\}}}{\Big(p-i\frac{1}{t_m}\Big)^2}dp, \tag{10}$$

and

8) G. NISHIMURA, *loc. cit.*

$$P'(p) = -i\left(\frac{1}{V}\right)^4 a^4 p^5 - 5\left(\frac{1}{V}\right)^3 a^3 p^4 - i21\left(\frac{1}{V}\right) a^2 p^3 + 48\left(\frac{1}{V}\right) a p^2 - i48p, \quad (11)$$

$$T'(p) = 2\left(\frac{1}{v}\right)^3 a^3 p^4 - i10\left(\frac{1}{v}\right)^2 a^2 p^3 - 24\left(\frac{1}{v}\right) a p^2 + i24p, \quad (12)$$

$$\psi'(p) = (p+a_1)(p+a_2)(p+a_3)(p+a_4)(p+a_5)(p+a_6), \quad (13)$$

$$\left.\begin{aligned} &a_1 = (\alpha_1 - i\beta_1)\frac{v}{a}, \quad a_2 = -(\alpha_1 + i\beta_1)\frac{v}{a}, \quad a_3 = (\alpha_2 - i\beta_2)\frac{v}{a}, \\ &a_4 = -(\alpha_2 + i\beta_2)\frac{v}{a}, \quad a_5 = (\alpha_3 - i\beta_3)\frac{v}{a}, \quad a_6 = -(\alpha_3 + i\beta_3)\frac{v}{a}, \\ &\alpha_1 = 0{\cdot}83199, \quad \alpha_2 = 2{\cdot}416332, \quad \alpha_3 = 0{\cdot}600844, \\ &\beta_1 = 2{\cdot}10618, \quad \beta_2 = 1{\cdot}040118, \quad \beta_3 = 0{\cdot}463744. \end{aligned}\right\} \quad (14)^{9}$$

where u_1, expressed by (8)a, corresponds to the longitudinal waves with velocity v; and where v_3, w_3 as expressed by (8)b, (8)c are due to the transversal waves with propagational velocity V, these two kinds of waves being of course propagated from the cavity as the result of the tractions applied. For evaluating the integrals (9), (10), as in the previous paper[10], we expand the integrants in expressions (9), (10) in partial fractions as in the following way:

$$\frac{P'(p)\, e^{1-ip\left\{\frac{1}{v}(r-a)\right\}}}{\psi'(p)\left(p-i\frac{1}{t_m}\right)^2} = \left\{ \frac{A_1}{(p+a_1)} + \frac{A_2}{(p+a_2)} + \frac{A_3}{(p+a_3)} + \frac{A_4}{(p+a_4)} + \frac{A_5}{(p+a_5)} + \frac{A_6}{(p+a_6)} + \frac{A_7}{\left(p-i\frac{1}{t_m}\right)^2} + \frac{A_8}{\left(p-i\frac{1}{t_m}\right)} \right\} e^{1-ip\left\{t-\frac{1}{v}(r-a)\right\}}, \quad (15)$$

$$\frac{T'(p)\, e^{1-ip\left\{t-\frac{1}{V}(r-a)\right\}}}{\psi'(p)\left(p-i\frac{1}{t_m}\right)^2} = \left\{ \frac{B_1}{(p+a_1)} + \frac{B_2}{(p+a_2)} + \frac{B_3}{(p+a_3)} + \frac{B_4}{(p+a_4)} + \frac{B_5}{(p+a_5)} + \frac{B_6}{(p+a_6)} + \frac{B_7}{\left(p-i\frac{1}{t_m}\right)^2} + \frac{B_8}{\left(p-i\frac{1}{t_m}\right)} \right\} e^{1-ip\left\{t-\frac{1}{V}(r-a)\right\}}, \quad (16)$$

9) H. KAWASUMI and R. YOSHIYAMA, *loc. cit.*
G. NISHIMURA, *loc. cit.*, p. 624.

10) G. NISHIMURA, *loc. cit.*, p. 625~626.

where the values A_1, A_2, A_3, A_4, A_5, A_6, A_7, A_8, B_1, B_2, B_3, B_4, B_5, B_6, B_7, B_8 are certain functions of the rapidity of the applied pressure $a/(t_m v)$. They are calculated for various values of $a/(t_m v)$ as in Tables I ~ II.

Table I.

$\frac{a}{t_m v}$	$\frac{A_1}{\left(\frac{a}{v}\right)^6}$	$\frac{A_2}{\left(\frac{a}{v}\right)^6}$	$\frac{A_3}{\left(\frac{a}{v}\right)^6}$	$\frac{A_4}{\left(\frac{a}{v}\right)^6}$	$\frac{A_5}{\left(\frac{a}{v}\right)^6}$	$\frac{A_6}{\left(\frac{a}{v}\right)^6}$	$\frac{A_7}{\left(\frac{a}{v}\right)^5}$	$\frac{A_8}{\left(\frac{a}{v}\right)^6}$
0·1	1·40366 +*i*0·09897	−1·40366 +*i*0·09897	−0·33440 −*i*0·14897	0·33440 −*i*0·14897	−0·09606 −*i*1·34530	0·09606 −*i*1·34530	−0·25755	2·79060
0·4	1·83968 −*i*0·09349	−1·83968 −*i*0·09349	−0·38639 −*i*0·07628	0·38639 −*i*0·07628	−1·48102 −*i*1·06214	1·48102 −*i*1·06214	−1·13793	2·46382
1·5	3·24787 −*i*5·35551	−3·24787 −*i*5·35551	−0·31132 +*i*0·26177	0·31132 +*i*0·26177	0·05050 +*i*0·46096	−0·05050 +*i*0·46096	−3·72826	9·26556
1·8	−0·07871 −*i*8·44732	0·07871 −*i*8·44732	−0·22840 +*i*0·30791	0·22840 +*i*0·30791	0·09597 +*i*0·29464	−0·09597 +*i*0·29464	−7·54750	15·68953
2·0	−5·54331 −*i*9·43054	5·54331 −*i*9·43054	−0·10839 +*i*0·34356	0·10839 +*i*0·34356	0·10177 +*i*0·21575	−0·10177 +*i*0·21575	−12·95040	17·74247
2·4	−8·39114 −*i*1·50698	8·39114 −*i*1·50698	−0·07065 +*i*0·31223	0·07065 +*i*0·31223	0·08576 +*i*0·13732	−0·08576 +*i*0·13732	−14·69639	2·11488
3·0	−3·14629 +*i*3·14862	3·14629 +*i*3·14862	0·02921 +*i*0·25255	−0·02921 +*i*0·25255	0·06271 +*i*0·07524	−0·06271 +*i*0·07524	−12·01904	−6·95280
3·5	−0·89240 +*i*2·35562	0·89240 +*i*2·35562	0·06920 +*i*0·19508	−0·06920 +*i*0·19508	0·04831 +*i*0·04990	−0·04831 +*i*0·04990	−8·92184	−5·20118
4·0	−0·17598 +*i*1·54125	0·17598 +*i*1·54125	0·08442 +*i*0·14590	−0·08442 +*i*0·14590	0·03793 +*i*0·03516	−0·03793 +*i*0·03516	−6·7827	−3·44459
5·0	0·11247 +*i*0·72339	−0·11247 +*i*0·72339	0·08188 +*i*0·07984	−0·08188 +*i*0·07984	0·02483 +*i*0·01984	−0·02483 +*i*0·01984	−4·38625	−1·64611
6·0	0·12099 +*i*0·40079	−0·12099 +*i*0·40079	0·06747 +*i*0·04456	−0·06747 +*i*0·04456	0·01738 +*i*0·01259	−0·01738 +*i*0·01259	−3·15434	−0·91586
8·0	0·07875 +*i*0·16999	−0·07875 +*i*0·16999	0·04266 +*i*0·01535	−0·04266 +*i*0·01535	0·00980 +*i*0·00629	−0·00980 +*i*0·00629	−1·96319	−0·38325
15·0	0·02195 +*i*0·03318	−0·02195 +*i*0·03318	0·01225 +*i*0·00022	−0·01225 +*i*0·00022	0·00277 +*i*0·00147	−0·00277 +*i*0·00147	−0·80560	−0·06975
20·0	0·01204 +*i*0·01682	−0·01204 +*i*0·01682	0·00672 −*i*0·00047	−0·00672 −*i*0·00047	0·00155 +*i*0·00079	−0·00155 +*i*0·00079	−0·56080	−0·03429

Table II.

$\frac{a}{t_m v}$	$\frac{B_1}{\left(\frac{a}{v}\right)^6}$	$\frac{B_2}{\left(\frac{a}{v}\right)^6}$	$\frac{B_3}{\left(\frac{a}{v}\right)^6}$	$\frac{B_4}{\left(\frac{a}{v}\right)^6}$	$\frac{B_5}{\left(\frac{a}{v}\right)^6}$	$\frac{B_6}{\left(\frac{a}{v}\right)^6}$	$\frac{B_7}{\left(\frac{a}{v}\right)^5}$	$\frac{B_8}{\left(\frac{a}{v}\right)^6}$
0·1	0·071886 +*i*0·01371	−0·071886 +*i*0·01371	−0·01253 −*i*0·02953	0·01253 −*i*0·02953	−0·42945 +*i*0·81951	0·42945 +*i*0·81951	0·13871	−1·60737
0·4	0·09565 +*i*0·00639	−0·09565 +*i*0·00639	−0·02019 −*i*0·02798	0·02019 −*i*0·02798	0·48074 +*i*1·15415	−0·48074 +*i*1·18415	0·77245	−2·26511
1·5	0·20051 −*i*0·25696	−0·20051 −*i*0·25696	−0·03559 −*i*0·00184	0·03559 −*i*0·00184	0·13689 −*i*0·28716	−0·13689 −*i*0·28716	0·61148	1·09191

(to be continued.)

Table II. (*continued.*)

	$\frac{B_1}{\left(\frac{a}{v}\right)^6}$	$\frac{B_2}{\left(\frac{a}{v}\right)^6}$	$\frac{B_3}{\left(\frac{a}{v}\right)^6}$	$\frac{B_4}{\left(\frac{a}{v}\right)^6}$	$\frac{B_5}{\left(\frac{a}{v}\right)^6}$	$\frac{B_6}{\left(\frac{a}{v}\right)^6}$	$\frac{B_7}{\left(\frac{a}{v}\right)^5}$	$\frac{B_8}{\left(\frac{a}{v}\right)^6}$
2·0	−0·16529 −*i*0·46241	0.16529 −*i*0·46241	−0·03018 +*i*0·01028	0·03018 +*i*0·01028	0·02334 −*i*0·16612	−0·02334 −*i*0·16612	−0·00032	1·23650
2·4	−0·42452 −*i*0·12907	0·42452 −*i*0·12907	−0·02319 +*i*0·01578	0 02319 +*i*0·01578	−0·00048 −*i*0·11105	0·00048 −*i*0·11105	−0·35601	0·44868
3·0	−0·18180 +*i*0·14353	0·18180 +*i*0 14358	−0 01322 +*i*0·01792	0·01322 +*i*0·01792	−0·00943 −*i*0·06652	0·00943 −*i*0·06652	−0·36713	−0·18984
3·5	−0·06049 +*i*0·11628	0·06049 +*i*0·11628	−0·00723 +*i*0·01663	0·00723 +*i*0·01663	−0·01018 −*i*0·04655	0·01018 −*i*0·04655	−0·27112	−0·17272
5·0	0·00140 +*i*0 03807	−0·00140 +*i*0·03807	0·00047 +*i*0·01001	−0·00047 +*i*0·01001	−0·00733 −*i*0·02054	0·00733 −*i*0·02054	−0·11750	−0·05509
6·0	0·00381 +*i*0·02145	−0·00381 +*i*0·02145	0·00166 +*i*0·00689	−0·00166 +*i*0·00689	−0·00560 −*i*0·01362	0·00560 −*i*0·01362	−0·07698	−0·02944
8·0	0·00303 +*i*0·00927	−0·00303 +*i*0·00927	0·00182 +*i*0·00353	−0·00182 +*i*0·00353	−0·00345 −*i*0·00720	0·00345 −*i*0·00720	−0·04018	−0·01119
15·0	0·00105 +*i*0·00174	−0·00105 +*i*0·00174	0·00078 +*i*0·00078	−0·00078 +*i*0·00078	−0·00108 −*i*0·00180	0·00108 −*i*0·00180	−0·01023	−0·00145
20·0	0·00053 +*i*0·00094	−0·00053 +*i*0·00094	0·00046 +*i*0·00137	−0·00046 +*i*0·00037	−0·00062 −*i*0·00102	0·00062 −*i*0·00102	−0·00556	−0·00059

Hence, by using relations (15), (16), it may be possible to evaluate the integrals (9), (10) by Cauchy's residue method. Then, after the necessary mathematical treatment, the wave-motions of particles that are some distance away from the cavity, owing to the longitudinal and transversal waves emanating from it, are expressed by

$$u_1 = u_{\text{free}} + u_{\text{forced}} + u_{\text{complementary}}, \tag{17}$$

$$v_3 = v_{\text{free}} + v_{\text{forced}} + v_{\text{complementary}}, \tag{18}$$

$$w_3 = w_{\text{free}} + w_{\text{forced}} + w_{\text{complementary}}, \tag{19}$$

where

$$\left.\begin{aligned} u_{\text{free}} &\approx -\frac{Pa}{27\mu}\left(\frac{a}{r}\right)\sin 2\theta\cos\phi\Big[\xi_1\exp\{-\beta_1\tau\}\sin(\alpha_1\tau+k_1) \\ &\qquad +\xi_2\exp\{-\beta_2\tau\}\sin(\alpha_2\tau+k_2) \\ &\qquad +\xi_3\exp\{-\beta_3\tau\}\sin(\alpha_3\tau+k_3)\Big], \quad \text{(a)} \\ u_{\text{forced}} &\approx -\frac{Pa}{27\mu}\left(\frac{a}{r}\right)\sin 2\theta\cos\phi\Big[\xi_4\tau\exp\{-\zeta\tau\}\Big], \quad \text{(b)} \\ u_{\text{complementary}} &\approx -\frac{Pa}{27\mu}\left(\frac{a}{r}\right)\sin 2\theta\cos\phi\Big[\xi_5\exp\{-\zeta\tau\}\Big], \quad \text{(c)} \end{aligned}\right\} \tag{20}$$

$$\left.\begin{aligned} v_{\text{free}} &\approx \frac{Pa}{27\mu}\left(\frac{a}{r}\right)\cos 2\theta\cos\phi\Big[\xi_1'\exp\{-\beta_1\tau'\}\sin(\alpha_1\tau'+k_1') \\ &\quad +\xi_2'\exp\{-\beta_2\tau'\}\sin(\alpha_2\tau'+k_2') \\ &\quad +\xi_3'\exp\{-\beta_3\tau'\}\sin(\alpha_3\tau'+k_3')\Big], \quad \text{(a)} \\ v_{\text{forced}} &\approx \frac{Pa}{27\mu}\left(\frac{a}{r}\right)\cos 2\theta\cos\phi\Big[\xi_4'\tau'\exp\{-\zeta\tau'\}\Big], \quad \text{(b)} \\ v_{\text{complementary}} &\approx \frac{Pa}{27\mu}\left(\frac{a}{r}\right)\cos 2\theta\cos\phi\Big[\xi_5'\exp\{-\zeta\tau'\}\Big], \quad \text{(c)} \end{aligned}\right\} \tag{21}$$

$$\left.\begin{aligned} w_{\text{free}} &\approx \frac{Pa}{27\mu}\left(\frac{a}{r}\right)\cos\theta\sin\phi\Big[\xi_1'\exp\{-\beta_1\tau'\}\sin(\alpha_1\tau'+k_1') \\ &\quad +\xi_2'\exp\{-\beta_2\tau'\}\sin(\alpha_2\tau'+k_2') \\ &\quad +\xi_3'\exp\{-\beta_3\tau'\}\sin(\alpha_3\tau'+k_3')\Big], \quad \text{(a)} \\ w_{\text{forced}} &\approx \frac{Pa}{27\mu}\left(\frac{a}{r}\right)\cos\theta\sin\phi\Big[\xi_4'\tau'\exp\{-\zeta\tau'\}\Big], \quad \text{(b)} \\ w_{\text{complementary}} &\approx \frac{Pa}{27\mu}\left(\frac{a}{r}\right)\cos\theta\sin\phi\Big[\xi_5'\exp\{-\zeta\tau'\}\Big]. \quad \text{(c)} \end{aligned}\right\} \tag{22}$$

In expressions (20), (21), (22),

$$\tau=\frac{v}{a}\left\{t-\frac{1}{v}(r-a)\right\}, \quad \tau'=\frac{v}{a}\left\{t-\frac{1}{V}(r-a)\right\}, \quad \zeta=\frac{a}{t_m v},$$

and the values α_1, α_2, α_3, β_1, β_2, β_3 are shown by (14). The valves ξ_1, ξ_2, ξ_3, ξ_4, ξ_5, ξ_1', ξ_2', ξ_3', ξ_4', ξ_5', k_1, k_2, k_3, k_1', k_2', k_3' are certain functions of $a/(t_m v)$, being numerically calculated for various values of $a/(t_m v)$, as shown in Tables III, IV.

Table III.

$a/(t_m v)$	ξ_1	ξ_2	ξ_3	ξ_4	ξ_5	k_1	k_2	k_3
0·1	−0·7650	0·1990	0·7340	−0·0700	0·7586	−0·0704	−0·4193	−1·500
0·4	−4·006	0·8566	3·962	−1·237	2·6789	0·0501	−1·950	−0·622
1·5	−51·091	3·320	−3·784	−15·20	37·780	1·0258	0·699	−1·462
2·0	118·942	3·918	−2·596	−70·406	96·459	−1·0398	1·2652	−1·130
2·4	111·246	4·176	−2·112	−95·878	13·797	−0·1773	1·3483	−1·015
3·0	72·594	4·142	−1·597	−98·014	−56·699	0·786	−1·4555	−0·876
3·5	47·932	−3·941	−1·322	−84·883	−49·485	1·2086	−1·230	−0.802
5·0	−19·898	−3·110	−0·858	−59·616	−22·373	−1·417	−0·773	−0·674
6·0	−13·654	−2·638	−0·700	−51·447	−14·937	−1·278	−0·584	−0·627
8·0	−8·148	−1·972	−0·5066	−42·692	−8·334	−1·137	−0·346	−0·571
15·0	−3·246	−0·9990	−0·2560	−32·848	−2·844	−0·986	−0·018	−0·488
20·0	−2·248	−0·7328	−0·189	−30·488	−1·864	−0·950	−0·070	−0·471

Table IV.

$a/(t_m v)$	ξ_1'	ξ_2'	ξ_3'	ξ_4'	ξ_5'	k_1'	k_2'	k_3'
0·1	−0·4134	0·1812	5·224	0·3920	−4·5395	−0·188	−1·170	1·0872
0·4	−2·160	0·802	−28·242	8·722	−25·588	−0·067	−0·946	−1·1762
1·5	−27·596	3·017	−26·942	25·904	46·256	0·908	−0·052	1·126
2·0	55·474	3·600	−18·952	−0·0181	69·843	−1·228	0·328	1·431
2·4	60·148	3·803	15·056	−24·130	30·412	−0·295	0·597	−1·567
3·0	39·246	3·774	11·387	−31·106	−16·084	0·6681	0·935	−1·430
3·5	25·918	3·588	9·422	−26·800	−17·073	1·091	1·161	−1·356
5·0	−10·760	−2·830	6·160	−16·592	−7·779	−1·534	−1·523	−1·228
6·0	−7·383	−2·402	4·985	−13·045	−4·989	−1·395	−1·334	−1·181
8·0	−4·406	−1·794	3·606	−9·078	−2·528	−1·255	−1·095	−1·124
15·0	−1·720	−0·932	1·7792	−4·334	−0·614	−1·029	−0·785	−1·029
20·0	−1·220	−0·6676	1·3488	−3.140	−0·3333	−1·06	−0·68	−1·025

As in Art. 2, expressions (17)∼(19) show that the longitudinal and transversal waves are of three kinds, namely, [1] free waves expressed by (20)a, (21)a, (22)a, [2] forced waves given by (20)b, (21)b, (22)b, and [3] complementary waves shown by (20)c, (21)c, (22)c. Naturally, the amplitudes of these three kinds of waves and also their phase-differences become certain functions of the rapidity of the pressure applied to the inner surface of the cavity. It will be seen, therefore, that the amplitudes of wave-motion of the particles that lie some distance away from the cavity vary with the rapidity of the applied pressure, and the apparent periods[11] of vibrations of the same particles in a state of initial motion also become certain functions of the value of $a/(t_m v)$. By using expressions (17)∼(19), we obtained Figs. 15∼27, in which are shown the radial, the co-latitudinal, and the azimuthal vibrations (u_1, v_3, w_3) of the particles due to the longitudinal and the transversal waves issuing from the cavity for various rapidities of the pressure applied. The units of the vertical scales in Figs. 15∼27 are taken as $\frac{Pa}{27\mu}\left(\frac{a}{r}\right)\sin 2\theta\cos\phi$, $\frac{Pa}{27\mu}\left(\frac{a}{r}\right)\cdot\cos 2\theta\cos\phi$, and $\frac{Pa}{27\mu}\left(\frac{a}{r}\right)\cos\theta\sin\phi$ for u_1, v_3, and w_3 respectively. It will be noticed from Figs. 15∼27 that the vibrations of particles, lying some distance away from the cavity, are of damped oscillations, which are the resultant oscillations obtained by adding the free, the forced, and the complementary waves. The maximum amplitudes of vibration

11) See p. 325 for definition of the apparent period of vibration of particle in a state of initial motion.

due to the longitudinal waves are usually smaller than those due to the transversal waves, and the apparent periods of vibration in a state of initial mtion due to the former waves are shorter than those due to the latter.

The curves U_1, V_3, and W_3 in Fig. 28, which are derived from

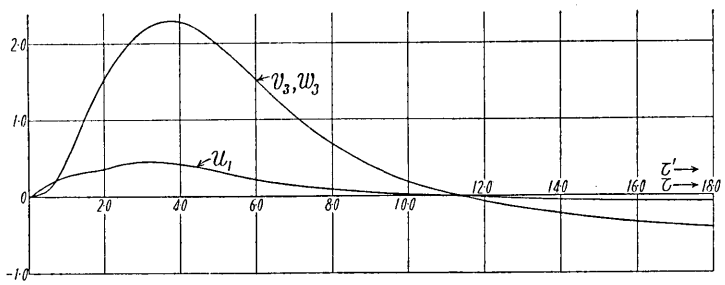

Fig. 15. $\frac{a}{t_m v} = 0{\cdot}10.$

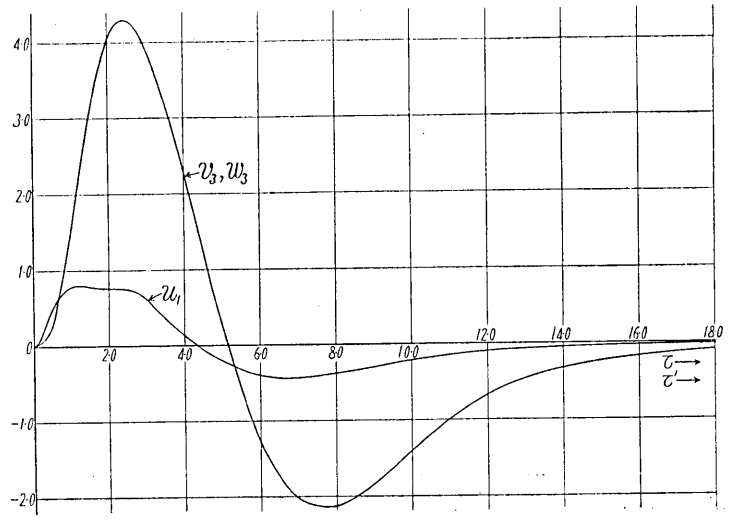

Fig. 16. $\frac{a}{t_m v} = 0{\cdot}40.$

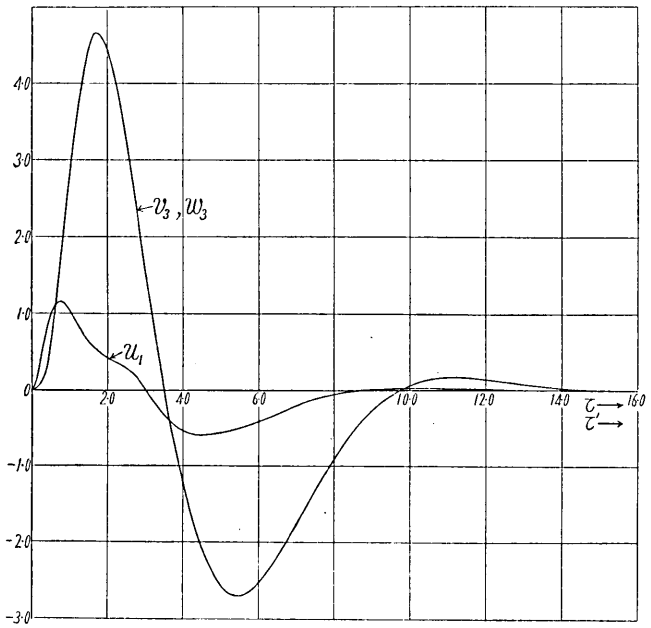

Fig. 17. $\frac{a}{t_m v} = 1{\cdot}0$.

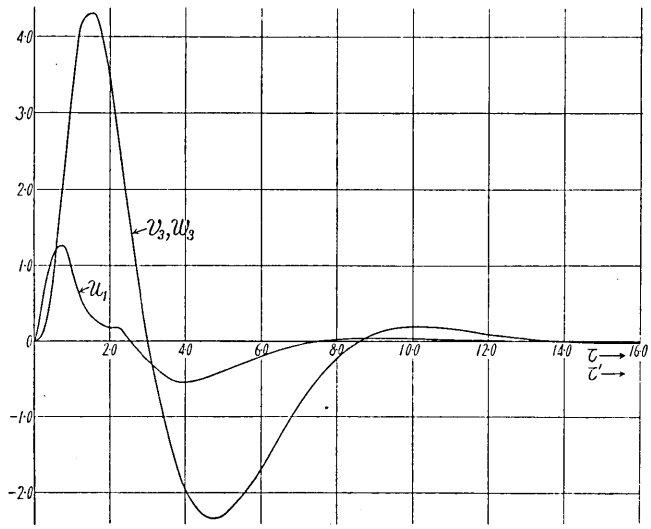

Fig. 18. $\frac{a}{t_m v} = 1{\cdot}5$.

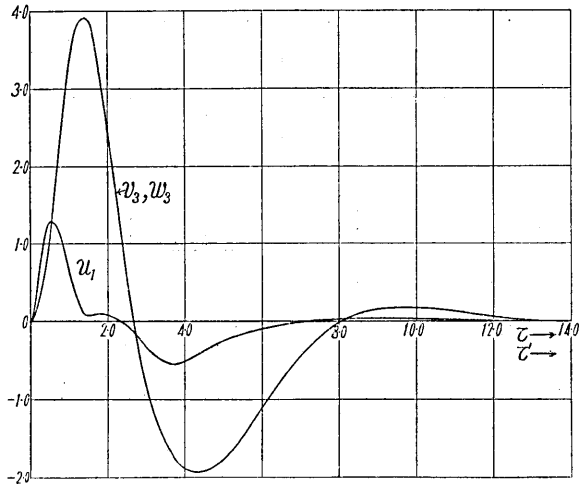

Fig. 19. $\frac{a}{t_m v} = 2{\cdot}0.$

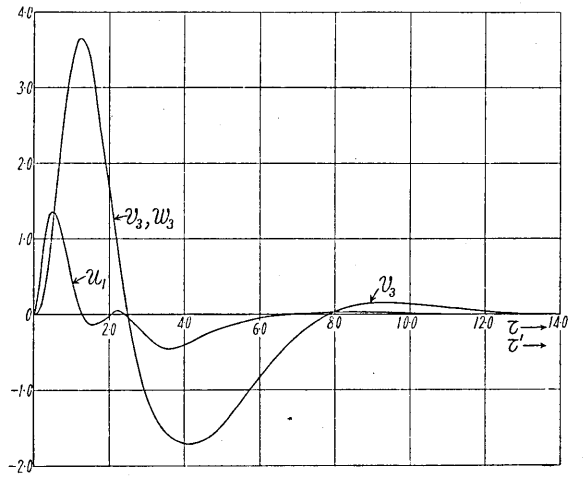

Fig. 20. $\frac{a}{t_m v} = 2{\cdot}4.$

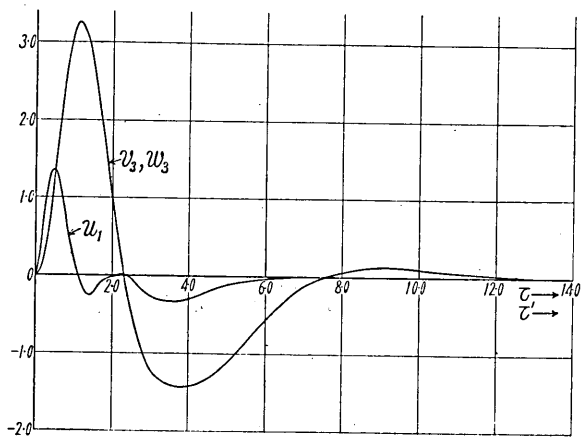

Fig. 21. $\frac{a}{t_m v} = 3{\cdot}0.$

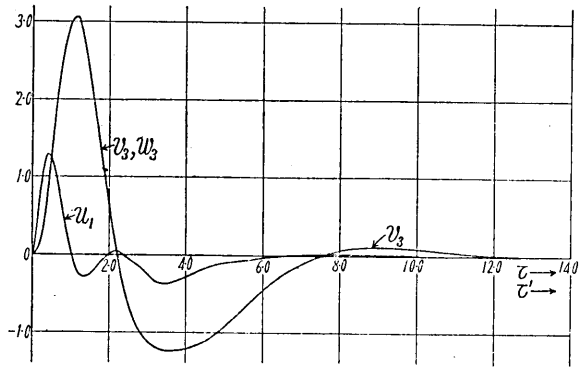

Fig. 22. $\frac{a}{t_m v} = 3{\cdot}5.$

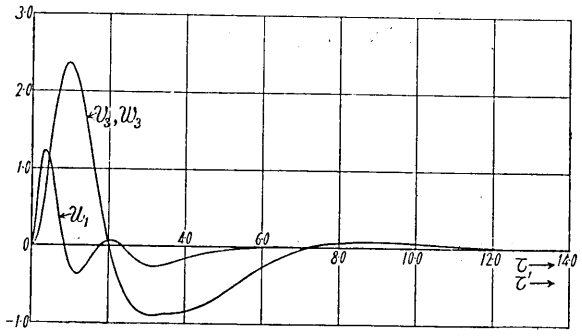

Fig. 23. $\frac{a}{t_m v} = 5{\cdot}0.$

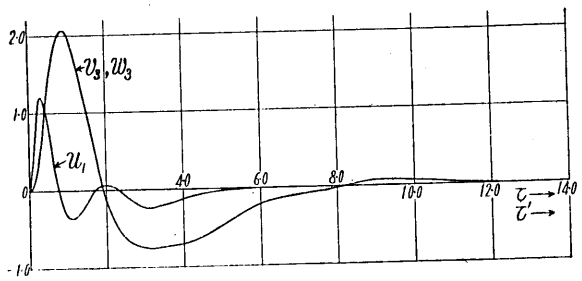

Fig. 24. $\frac{a}{t_m v} = 6{\cdot}0.$

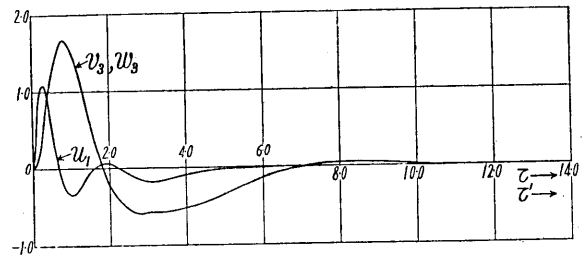

Fig. 25. $\frac{a}{t_m v} = 8{\cdot}0.$

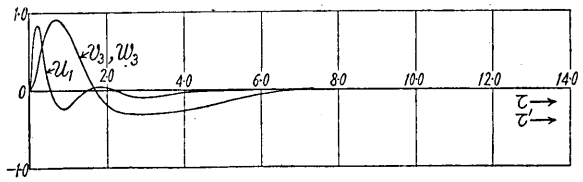

Fig. 26. $\frac{a}{t_m v} = 15{\cdot}0.$

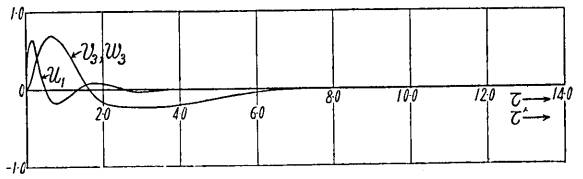

Fig. 27. $\frac{a}{t_m v} = 20{\cdot}0.$

Figs. 15~27, show the displacement-amplitudes of vibration of particles in a state of initial motion due to the longitudinal and transversal waves, the absissa in Fig. 28 being the value of the rapidity of the pressure applied. As in Art. 2, we can also see the spectrum-like nature of the two curves U_1 and V_3, Fig. 28, although the variation in the former curve with rapidity is less pronounced than in that of the latter, whence it will be seen that when the value $a/(t_m v)$ greatly exceeds 20, the displacement-amplitudes due to both waves will be nil, and the maximum displacement-amplitude in a state of initial motion due to the transversal wave will be smaller than those due to the longitudinal wave. Since when $a/(t_m v)$ becomes zero, the problem becomes one of statics, we cannot see any wave-motion of the particles that lie some distance away from the cavity. Fig. 29 shows the variation in the ratio of the two curves U_1, V_3, Fig. 28; the ratio becomes maximum when $a/(t_m v)$ becomes approximately unity, and when $a/(t_m v)$ greatly exceeds 20, it will be smaller than unity.

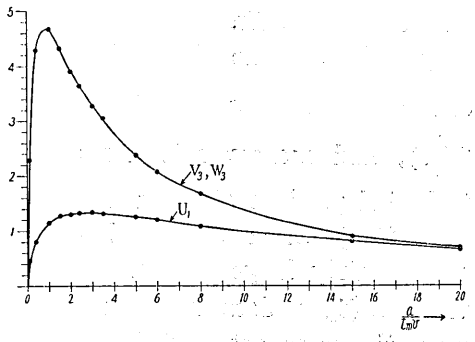

Fig. 28.

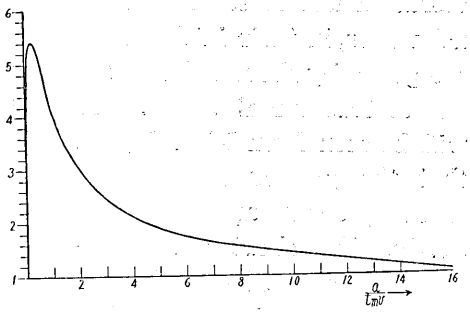

Fig. 29.

Curves T_1 and T_1', Fig. 30, which are derived from Figs. 15~27, show the durations of time from the beginning of the vibration until we come to the first nil of the displacement-amplitude; the curve T_1 corresponds to the case of radial vibrations due to the longitudinal wave, while curve T_1' is the case of the azimuthal or co-latitudinal vibrations due to the transversal waves. Curves T_2 and T_2', Fig. 31, show the durations of time from the begin-

12) H. Honda and others have studied the vibration of particle due to the forced wave emanating from a spherical cavity in the stationary state for the case when the the pressure-variation on the inner surface of the cavity has the same space-distribution as in the present article, although the time-factor of the applied pressure is simple-harmonic, like e^{ipt}. Taking the value of L/a as abscissa, they obtained the ratio-curve of the vibration-amplitude of particles, lying some distance away from the cavity, and due to the longitudinal and transversal waves emanating from it. Their study, however, is restricted to the case of forced waves. H. Honda, T. Miura, *Kensin-Zihô*, **10** (1937).

ning of the vibration to the time when the second nil of the displacement-amplitude occurs, the two corresponding respectively to the vibrations due to the longitudinal and the transversal waves. It will be seen from Figs. 30, 31, that when $a/(t_m v)$ is small, the difference between the apparent periods of the respective vibrations in their initial states due to the transversal and the longitudinal waves is very small, although it becomes as large as $1{\cdot}2\frac{v}{a}t$ (or $6\frac{v}{a}t$), and moreover it seems to be independent of the value of $a/(t_m v)$ when $a/(t_m v)$ becomes fairly large. When the value $a/(t_m v)$ does not equal zero, the apparent periods of vibration due to the longitudinal waves, in their initial state, are generally shorter than those due to transversal waves. It will be seen from Figs. 30, 31, that the greater the rapidity of the pressure applied to the cavity, the shorter the apparent periods of vibrations in the state of initial motion. Even if the rapidity $a/(t_m v)$ becomes very large, neither seem to vary so much as the period of vibration due to forced waves as in Art. 2. The fact that the relation between both the apparent periods and the rapidity of the applied pressure is not so simple as in the case of forced waves, is obviously due to the presence of both free and initial waves in addition to the forced wave, as will be seen from expressions (20), (21), (22).

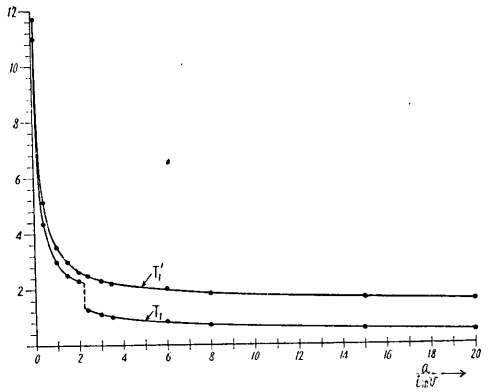

Fig. 30.

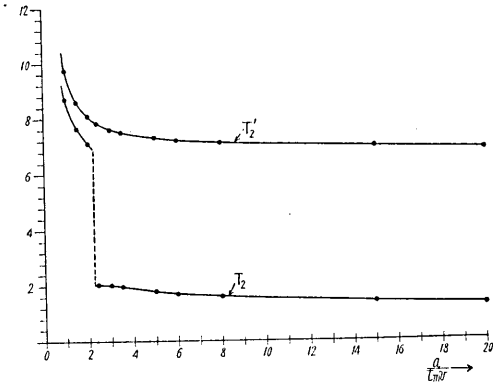

Fig. 31.

Now, from Fig. 30, we can easily obtain the curve T_s/T_p in Fig. 32, which shows the ratio of the apparent half-period of vibration T_s due to transversal waves to T_p due to the longitudinal waves. The ratio T_s/T_p, which is slightly larger than unity when the rapidity is small, becomes from 2·0 to 3·0 even if it becomes fairly large. Letting

both the wave-lengths of the longitudinal and the transversal waves in the state of their initial motions be L_p, L_s respectively, we obtain the relations,

$$L_p = vT_p, \quad L_s = VT_s,$$

where v, V are the velocities of both waves, so that when Poisson's ratio is 1/4,

$$L_s/L_p = (1/1{\cdot}732)\ (T_s/T_p).$$

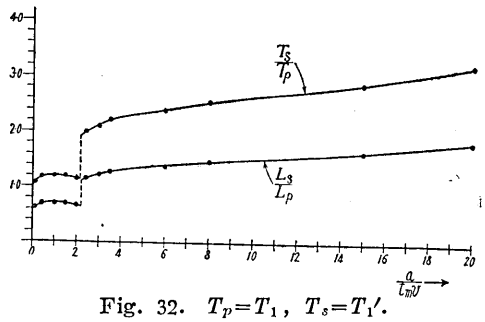

Fig. 32. $T_p=T_1$, $T_s=T_1'$.

The ratio L_s/L_p for the present case is also shown in Fig. 32, which ratio is proportional to the value of T_s/T_p, and is certain function of the rapidity of the applied stress. It is remarkable that the ratio L_s/L_p, which is less than unity when the rapidity is small, is from 1·0 to 2·0 even if $a/(t_m v)$ be fairly large. By using the curves of the apparent periods shown in Fig. 31, it may be possible to obtain the curves T_s/T_p, L_s/L_p, like those in Fig. 32, although the qualitative character of the two ratios T_s/T_p, L_s/L_p relating to variation in the value $a/(t_m v)$ do not differ much from those shown in Fig. 32.

By studying the deep-focus earthquake of Feb. 20, 1931, T. Ishikawa[13] found that the ratio T_s/T_p is nearly equal to 1·77, and that $L_s = L_p$ for that earthquake, and further that the displacement of particles near the earthquake-origin in the case of a deep-focus earthquake is usually quicker than that in the case of a shallow earthquake. From Fig. 32, we can see that when the rapidity of the applied pressure is fairly large, the ratios T_s/T_p, L_s/L_p are respectively 2, 1·2, the two values being of the same order as those of Ishikawa. So that it may be in order to conclude that the seismic waves, in the case of deep-focus earthquake, may be propagated from a cavity, the inner surface of which is subjected to a pressure of shock type, as assumed in the present Article.

The writers regret here that the theoretical results thus obtained of the periods of vibration due to the longitudinal and the transversal waves are not strictly borne out by seismometrical studies of actual earthquakes, and they fervently hope that experimenters will not be long in verifying their theoretical results with the aid of seismometrical results with actual deep-focus earthquakes; for to use the data of deep-focus earthquakes may not only be more reasonable, but is more

13) T. Ishikawa, *Jour., Met. Soc., Japan*, **10** (1932), 252.

convenient than to use the data of shallow earthquakes.

Applying their mathematical results to seismometrical observations of seven deep-focus earthquakes, H. Honda[14] and T. Miura found that in the matter of vibration-amplitudes of the initial motion due to both *P*- and *S*-waves, it may be more consistent with the facts of seismometry to take a cavity of radius, say, $9\sim11$ km as a model in connexion with the origin of deep-focus earthquakes rather than to assume a point as origin, as H. Kawasumi, and W. Inouye[15] have already pointed out theoretically in their papers. H. Honda[16] found, moreover, that the distributions of vibration-amplitudes of the initial-motion on the earth's surface due to the *P*- and *S*-waves in the case of certain deep-focus earthquakes, are fairly consistent with the theoretical distribution of vibration-amplitudes obtained by him under the assumption that the forced waves emerge from a cavity, to which inner surface the following stresses are applied:

$$\widehat{rr}_{r=a}=F\sin2\theta\cos\phi\cdot\sin pt,\ \widehat{r\theta}_{r=a}=\widehat{r\phi}_{r=a}=0,$$

in which the surface-distributions are the same as those in the present Article, although the time-factor differs from expression (7) assumed in this paper. Therefore, assuming the deep-focus earthquakes examined by H. Honda to be generated by a pressure with the time-variation expressed by (7), we obtain the values of $a/(t_m v)$ for earthquakes Nos. 1, 2, as shown in the seventh column in Table V[17]. (The period of

Table V.

No.	time of occurrence	Hypocenter		focal-depth	period of *P*-wave	Amplitude factor of *P*-wave	$\frac{a}{t_m v}$	$\frac{v}{a}t$
		longi-tude	Lati-tude					
1	June, 3, 1929	137·2°	34·3°	320 km	3·5 sec	$4{\cdot}95\times10^5\text{cm}^2$	2·2	2·04 or 7
2	June, 30, 1931	136·5°	34·2°	360 km	2·5 sec	$1{\cdot}54\times10^5\text{cm}^2$	3·0	2

earthquake No. 1 was obtained by H. Honda, and that of No. 2 by H. Morita.) As the ordinates of the curve, Fig. 29, were obtained experimentally by Honda, we easily obtain the values $a/(t_m v)$ of the abscissa

14) H. HONDA, and T. MIURA, *loc. cit.*

15) H. KAWASUMI and R. YOSHIYAMA, *loc, cit.* W. INOUYE, *Bull. Earthq. Res. Inst.*, **14** (1936), 582; **15** (1937), 90.

16) H. HONDA, *Geophy. Mag.*, **8** (1934), 153.

17) Since the periods of the *P*-wave of the other five earthquakes (No. 3~7) are not given iu Honda's paper, we shall reserve our discussion of them for an other occasion.

in Fig. 29, as shown in Table V. Therefore, from Fig. 31, we obtain the values vt/a, which give the apparent periods of the initial motion due to the longitudinal waves in the cases of $a/(t_m v)=2{\cdot}2$, $a/(t_m v)=3{\cdot}0$, as shown in the eighth column in Table V, and by using the velocity of the longitudinal wave, which is 8·8 km/sec, as assumed by Honda, we obtain the dimensions of the cavities, namely, for earthquake No. 1, $a=15{\cdot}8$ or 4·4 km, and for earthquake No. 2, $a=11$ km. These dimensions, however, differ somewhat from those given by Honda[18]. Next, by equating both the theoretical and experimental amplitudes of the initial-motions for the respective cases in which $a/(t_m v)=2{\cdot}2$, 3·0, we get the equations, $1{\cdot}32\, P_m a^2/(27\mu)=4{\cdot}94\times10^5\,\mathrm{cm}^2$ for earthquake No. 1, and $1{\cdot}34\, P_m a^2/(27\mu)=1{\cdot}54\times10^5\,\mathrm{cm}^2$ for earthquake No. 2. The values of the left-hand terms of both equations are obtained from ordinates of the curve U_1 in Fig. 28; and those of the right-hand terms are shown in the sixth column of Table V. Then, assuming $\mu=8{\cdot}4\times10^{11}$ dynes/cm^{-2}, we obtain $P_m=3{\cdot}4\times10^6$ or $4{\cdot}4\times10^7$ dynes/cm^2 for earthquake No. 1, and $P_m=2{\cdot}1\times10^6$ dynes/cm^2 for earthquake No. 2. Lastly, the values t_m for both earthquakes No. 1 and No. 2 are easily calculated by using the values of a, v, namely, $t_m=0{\cdot}818$ or 0·227 sec for earthquake No. 1, and $t_m=0{\cdot}416$ sec. for earthquake No. 2.

In other words, we have found it possible to make the results of seismometrical observations of deep-earthquake No. 1, which particularly concerns both vibration-amplitude and direction of motion of the particles on the earth's surface in the state of their initial motions due to both P- and S-waves, consistent with the results that were obtained by a mathematical study of the same earthquake wherein the following reasonable assumptions were made, namely, that seismic waves, both longitudinal and transversal, emanate from a cavity, the radius of which is 15·8 or 4·4 km, at a depth of 320 km from the earth's surface as the result of pressure applied normal to its inner surface. This pressure, which has a distribution of $P_2^1(\cos\theta)\cdot\cos\phi$ on the inner surface of the cavity, reaches maximum $P_m=4{\cdot}4\times10^7$ dyne/cm^2 at $t_m=0{\cdot}8$ or 0·2 sec., after its variation begins, which accords with the time-variation expressed by $\frac{t}{t_m}\exp\{1-t/t_m\}$. It is also possible to explain the mechanism of occurrence of earthquake No. 2, which explanation harmonizes with experimental results, the following data being assumed:

Focal depth $=360$ km, $a=11$ km, $P_m=2{\cdot}1\times10^6$ dynes/cm^2, $t_m=0{\cdot}4$ sec.

18) The dimensions obtained by Honda are 11 km and 9 km for earthquakes Nos. 1, 2 respectively. H. HONDA and T. MIURA, *loc. cit.*

To summarize, we have obtained from the present calculations, the following facts which in no way conflict with the results of seismometrical observations, namely, that certain deep-focus earthquakes result from pressure of shock-type, which acts on the inner surface of a spherical cavity in the earth, and of which the time when its maximum occurs is less than one second. The dimension of the spherical cavity range from a few tens of kilometers to a few kilometers, the distance of its center from the earth's surface being a few hundred kilometers.

Since from the data given by Honda and others, it is not possible to know the apparent vibration-periods of particles due to the transversal (S-) wave, should both the apparent periods of vibrations in the condition of initial motion due to P-and S-waves determined experimentally for the various kinds of deep-earthquakes, then by assuming a more favourable time-variation in the traction applied to the cavity, it may be possible to trace more accurately the mechanism of deep-earthquake occurrence. As already discussed, we hope that experimenters will do all in their power to determine these periods to enable not only an understanding of the mechanism of earthquake occurrence, but also to give us an idea of the exact nature of seismic waves in the earth's crust.

In concluding Art. 3, the writers shall enumerate some of the ideas that they have on the question of the origin of earthquakes. As is well known, when a great earthquake occurs, the epicentral region of the earth's crust is subjected to severe seismal vibrations, mainly as the result of seismic wave-energy propagated from the earthquake origin, causing permanent crustal deformations in the region affected, accompanied sometimes with considerable dislocations. If we assume the necessity of invoking a mechanical force to explain the origin of earthquakes with all its attendant phenomena, for example, the wave-motions of particles in the earth, crustal deformations, ground cracks, dislocations, etc., it is possible to roughly calculate the energy of an earthquake in the earth, the crust of which is composed of plastico-elastic material. For example, by applying a force of a certain magnitude at the origin of an earthquake, some energy may be imparted to the earth's crust. A part of the work thus done by the force may be consumed in straining the earth's plastic crust, which is irreversible, and the remainder of the work may be stored as elastic strain energy. The former strain may appear as crustal deformations of permanet set, while the latter strain energy may be transformed into surface energy as the result of the occurrence of earthquake cracks, besides changing into seismic wave-energy at the instant of the earthquake. In other words,

The work done by force
- Straining the plastic earth—Crustal deformation of permant set.
- Elastic strain energy
  - Surface energy of crack.
  - Seismic wave-energy.

The work consumed in crustal deformation may be roughly calculated by modifying the theory[19] obtained by one of the present writers, and the surface energy due to the appearance of earthquake cracks in the earth's crust may also be calculated by suitably assuming the area of cracks, the wave-energy being assumed from the theory given in this paper.

4. When the stresses on the inner surface of a spherical cavity in an elastic earth are expressed by co-latitudinal and azimuthal distributions, such as

$$\left.\begin{aligned} \widehat{rr}_{r=a} &= 0, \\ \widehat{r\theta}_{r=a} &= f(t)\cos 2\theta\cos\phi, \\ \widehat{r\phi}_{r=a} &= -f(t)\cos\theta\sin\phi, \end{aligned}\right\} \tag{23}$$

then the diverging waves that emanate from the cavity become two bodily waves, the longitudinal and transversal, as in the case of Art. 3, and the particles that are some distance away from the cavity assume the following vibrational motions of the radial, co-latitudinal, and azimuthal displacements (u_1, v_3, w_3) in the elastic earth, the Poisson ratio of which is 1/4:

$$u_1 \fallingdotseq -\frac{3}{\pi}\frac{V^6}{\mu v a^3}\frac{1}{r}\int_{-\infty}^{\infty} K'(p)\frac{P''(p)e^{ip\left\{t-\frac{1}{v}(r-a)\right\}}}{\psi'(p)}\sin 2\theta\cos\phi\, dp, \tag{24}$$

$$v_3 \fallingdotseq -\frac{1}{2\pi}\frac{V^3v^2}{\mu a^3}\frac{1}{r}\int_{-\infty}^{\infty} K'(p)\frac{Q''(p)e^{ip\left\{t-\frac{1}{v}(r-a)\right\}}}{\psi'(p)}\cos 2\theta\cos\phi\, dp, \tag{25}$$

$$w_3 \fallingdotseq \frac{1}{2\pi}\frac{V^3v^2}{\mu a^3}\frac{1}{r}\int_{-\infty}^{\infty} K'(p)\frac{Q''(p)e^{ip\left\{t-\frac{1}{v}(r-a)\right\}}}{\psi'(p)}\cos\theta\sin\phi\, dp, \tag{26}$$

where

$$K'(p)=\int_{-\infty}^{\infty} f(\lambda)e^{-ip\lambda}d\lambda, \tag{27}$$

19) G. NISHIMURA, *Bull. Earthq. Res. Inst.*, **12** (1934), 368~401.

$$P''(p) = -\left(\frac{a}{V}\right)^3 p^4 + i5\left(\frac{a}{V}\right)^2 p^3 + 12\left(\frac{a}{V}\right)p^2 - i12p, \tag{28}$$

$$Q''(p) = -i3\left(\frac{a}{v}\right)^4 p^5 - 13\left(\frac{a}{v}\right)^3 p^4 + i37\left(\frac{a}{v}\right)^2 p^3 + 72\left(\frac{a}{v}\right)p^2 - i72p, \tag{29}$$

and $\psi'(p)$ has the the same expressision as (13) in Art. 3. As in the case of Art. 3, the amplitudes of the co-latitudinal and the azimuthal components of displacements of the longitudinal wave are less than the radial component of displacement (u_1) of that wave, and those of the radial component of displacement due to the transversal wave are also less than those of the co-latitudinal and the azimuthal components of displacements (v_3, w_3) due to the same wave. We, therefore, ignore these small displacements in studying the wave-motions of particles that are some distance away from the cavity.

By letting the time-factor $f(t)$ be

$$\left.\begin{aligned} f(t) &= T\frac{t}{t_m}\exp\{1-t/t_m\}, \\ \text{when } t\geqq 0, \text{ and} \quad f(t) &= 0, \end{aligned}\right\} \tag{30}$$

when $t\leqq 0$, we obtain the following expression of displacement from expressions (24), (25), (26):

$$u_1 \approx \frac{3}{\pi}\frac{V^6}{\mu v a^3} T\frac{1}{r}\sin 2\theta\cos\phi\cdot X'\left\{t-\frac{1}{v}(r-a)\right\}, \tag{31}$$

$$v_3 \approx \frac{1}{2\pi}\frac{V^3 v^2}{\mu a^3} T\frac{1}{r}\cos 2\theta\cos\phi\cdot Y'\left\{t-\frac{1}{V}(r-a)\right\}, \tag{32}$$

$$w_3 \approx \frac{-1}{2\pi}\frac{V^3 v^2}{\mu a^3} T\frac{1}{r}\cos\theta\sin\phi\cdot Y'\left\{t-\frac{1}{V}(r-a)\right\}, \tag{33}$$

where

$$X'\left\{t-\frac{1}{v}(r-a)\right\} = \frac{1}{t_m}\int_{-\infty}^{\infty}\frac{P''(p)}{\psi'(p)}\frac{e^{1-ip\left\{t-\frac{1}{v}(r-a)\right\}}}{\left\{p-i\frac{1}{t_m}\right\}^2}dp, \tag{34}$$

$$Y'\left\{t-\frac{1}{V}(r-a)\right\} = \frac{1}{t_m}\int_{-\infty}^{\infty}\frac{Q''(p)}{\psi'(p)}\frac{e^{1-ip\left\{t-\frac{1}{V}(r-a)\right\}}}{\left\{p-i\frac{1}{t_m}\right\}^2}dp. \tag{35}$$

Applying the same method as in Art. 3, we expand the integrants of

the integrals (34), (35) for evaluating these integrals, as follows:

$$\frac{P''(p)e^{1-ip\left\{t-\frac{1}{v}(r-a)\right\}}}{\psi'(p)\cdot\left(p-i\frac{1}{t_m}\right)^2}=\left\{\frac{C_1}{(p+a_1)}+\frac{C_2}{(p+a_2)}+\frac{C_3}{(p+a_3)}+\frac{C_4}{(p+a_4)}+\frac{C_5}{(p+a_5)}+\frac{C_6}{(p+a_6)}+\frac{C_7}{\left(p-i\frac{1}{t_m}\right)^2}+\frac{C_8}{\left(p-i\frac{1}{t_m}\right)}\right\}e^{1-ip\left\{t-\frac{1}{v}(r-a)\right\}}, \quad (36)$$

$$\frac{Q''(p)e^{1-ip\left\{t-\frac{1}{V}(r-a)\right\}}}{\psi'(p)\cdot\left(p-i\frac{1}{t_m}\right)^2}=\left\{\frac{D_1}{(p+a_1)}+\frac{D_2}{(p+a_2)}+\frac{D_3}{(p+a_3)}+\frac{D_4}{(p+a_4)}+\frac{D_5}{(p+a_5)}+\frac{D_6}{(p+a_6)}+\frac{D_7}{\left(p-i\frac{1}{t_m}\right)^2}+\frac{D_8}{\left(p-i\frac{1}{t_m}\right)}\right\}e^{1-ip\left\{t-\frac{1}{V}(r-a)\right\}}. \quad (37)$$

Table VI.

$\frac{a}{t_m v}$	$\frac{C_1}{\left(\frac{a}{v}\right)^6}$	$\frac{C_2}{\left(\frac{a}{v}\right)^6}$	$\frac{C_3}{\left(\frac{a}{v}\right)^6}$	$\frac{C_4}{\left(\frac{a}{v}\right)^6}$	$\frac{C_5}{\left(\frac{a}{v}\right)^6}$	$\frac{C_6}{\left(\frac{a}{v}\right)^6}$	$\frac{C_7}{\left(\frac{a}{v}\right)^5}$	$\frac{C_8}{\left(\frac{a}{v}\right)^6}$
0·1	−0·23588 +*i*0·01092	0·23588 +*i*0·01092	0·12073 −*i*0·02616	−0·12073 −*i*0·02616	−0·00642 −*i*0·33298	0·00642 −*i*0·33298	−0·06435	0·69644
0·4	−0.30480 +*i*0·05150	0·30480 +*i*0·05150	0·12040 −*i*0·05622	−0·12040 −*i*0·05622	−0·35168 −*i*0·28097	0·35168 −*i*0·28097	−0·27999	0·57139
1·0	−0·4957 +*i*0·3036	0·4957 +*i*0·3036	0·0859 −*i*0·1123	0·0859 −*i*0·1132	−0·1380 +*i*0·2124	0·1380 +*i*0·2124	−0·1405	−0·8058
1·5	−0·43676 +*i*0·95603	0·43676 +*i*0·95603	0·03259 −*i*0·13331	−0·03259 −*i*0·13331	0·00654 +*i*0·11434	−0·00654 +*i*0·11434	0·48329	−1·87412
2·0	1·0790 +*i*1·4831	−1·0790 +*i*1·4831	−0·0273 −*i*0·1253	0·0273 −*i*0·1253	0·0209 +*i*0·0577	−0·0209 +*i*0·0577	2·0668	−2·8311
3·0	0·46295 −*i*0·58624	−0·46295 −*i*0·58624	−0·05827 −*i*0·06293	0·0527 −*i*0·06293	0·01450 +*i*0·01937	−0·01450 +*i*0·01937	1·70255	1·25960
5·0	−0·03286 −*i*0·11837	0·03286 −*i*0·11837	−0·03820 −*i*0·00542	0·03820 −*i*0·00542	0·00587 +*i*0·00521	−0·00587 +*i*0·00521	0·44850	0·23717
8·0	−0·01645 −*i*0·02679	0·01645 −*i*0·02679	−0·01467 +*i*0·00432	0·01467 +*i*0·00432	0·00234 +*i*0·00167	−0·00234 +*i*0·00167	0·13499	0·04160
11·0	−0·00851 −*i*0·01108	0·00851 −*i*0·01108	−0·00702 +*i*0·00361	0·00702 +*i*0·00361	0·00124 +*i*0·00075	−0·00124 +*i*0·00075	0·06267	0·01343
15·0	−0·00458 −*i*0·00489	0·00458 −*i*0·00489	−0·00341 +*i*0·00231	0·00341 +*i*0·00231	0·00068 +*i*0·00062	−0·00068 +*i*0·00026	0·03059	0·00463

Table VII.

$\frac{a}{t_m v}$	$\frac{D_1}{\left(\frac{a}{v}\right)^6}$	$\frac{D_2}{\left(\frac{a}{v}\right)^6}$	$\frac{D_3}{\left(\frac{a}{v}\right)^6}$	$\frac{D_4}{\left(\frac{a}{v}\right)^6}$	$\frac{D_5}{\left(\frac{a}{v}\right)^6}$	$\frac{D_6}{\left(\frac{a}{v}\right)^6}$	$\frac{D_7}{\left(\frac{a}{v}\right)^6}$	$\frac{D_8}{\left(\frac{a}{v}\right)^8}$
0·1	0·14692 +i0·01071	−0·14692 +i0·01071	−0·11152 +i0·06657	0·11152 −i0·06657	1·39651 −i2·36155	−1·39651 −i2·36155	−0·41652	4·83483
0·4	0·19364 −i0·01007	−0·19364 −i0·01007	−0·13288 −i0·04295	0·13288 −i0·04295	−1·24767 −i3·49078	1·24767 −i3·49078	−2·35363	7·08760
1·0	0·3294 −i0·1516	−0·3294 −i0·1516	−0·1473 +i0·0253	0·1473 +i0·0253	−1·8870 +i0·8910	1·8870 +i0·8910	−3·7206	−1·5294
1·5	0·34097 −i0·5602	−0·34097 −i0·56022	−0·12073 +i0·07904	−0·12073 +i0·17904	−0·44914 +i0·82948	0·44914 +i0·82948	−3·02683	−0·69660
2·0	−0·8241 −i1·1659	0·8241 −i1·1659	−0·0559 +i0·1124	0·0559 +i0·1124	−0·0935 +i0·4861	0·0935 +i0·4861	−3·7109	1·1349
3·0	−0·33001 +i0·32916	0·33001 +i0·32916	0·00039 +i0·09019	0·00039 +i0·09019	0·01779 +i0·19842	−0·01779 +i0·19842	−2·47810	−1·23555
5·0	0·01168 +i0·07574	−0·01168 +i0·07574	0·02547 +i0·03159	−0·02547 +i0·09019	0·01856 +i0·06193	−0·01856 +i0·06193	−1·08562	−0·33853
8·0	0·00820 +i0·01782	−0·00820 +i0·01782	0·01438 +i0·00720	−0·01438 +i0·00720	0·00912 +i0.02185	−0·00912 +i0·02185	−0·54558	−0·09375
15·0	0·00210 +i0·00358	−0·00210 +i0·00358	0·00429 +i0·00057	−0·00429 +i0·00057	0·00292 +i0·00561	−0 00292 +i0·00561	−0·24388	−0·01954

The values $C_1 \sim C_8$, $D_1 \sim D_8$, thus obtained, which become certain functions of $a/(t_m v)$, are numerically calculated for various values of $a/(t_m v)$, as shown in Tables VI, VII. Then, by using (36), (37), we obtain the following expressions for thc wave-motions of particles that are some distance away from the cavity, from expressions (31)$\sim$(33), by applying Cauchy's residue methode on (34), (35):

$$u_1 = u_{\text{free}} + u_{\text{forced}} + u_{\text{complementary}}, \tag{38}$$

$$v_3 = v_{\text{free}} + v_{\text{forced}} + v_{\text{complementary}}, \tag{39}$$

$$w_3 = w_{\text{free}} + w_{\text{forced}} + w_{\text{complementary}}, \tag{40}$$

where

$$\left.\begin{aligned} u_{\text{free}} &\approx \frac{Ta}{27\mu}\left(\frac{a}{r}\right)\sin 2\theta \cos\phi \Big[\eta_1 \exp\{-\beta_1\tau\} \sin(\alpha_1\tau + \kappa_1) \\ &\qquad + \eta_2 \exp\{-\beta_2\tau\} \sin(\alpha_2\tau + \kappa_2) \\ &\qquad + \eta_3 \exp\{-\beta_3\tau\} \sin(\alpha_3\tau + \kappa_3) \Big], \qquad \text{(a)} \\ u_{\text{forced}} &\approx \frac{Ta}{27\mu}\left(\frac{a}{r}\right)\sin 2\theta \cos\phi \Big[\eta_4 \tau \exp\{-\zeta\tau\} \Big], \qquad \text{(b)} \\ u_{\text{complementary}} &\approx \frac{Ta}{27\mu}\left(\frac{a}{r}\right)\sin 2\theta \cos\phi \Big[\eta_5 \exp\{-\zeta\tau\} \Big], \qquad \text{(c)} \end{aligned}\right\} \tag{41}$$

$$\left.\begin{aligned} v_{\text{free}} &\approx \frac{Ta}{27\mu}\left(\frac{a}{r}\right)\cos 2\theta\cos\phi\Big[\eta_1'\exp\{-\beta_1\tau'\}\sin(\alpha_1\tau'+\kappa_1') \\ &\qquad +\eta_2'\exp\{-\beta_2\tau'\}\sin(\alpha_2\tau'+\kappa_2') \\ &\qquad +\eta_3'\exp\{-\beta_3\tau'\}\sin(\alpha_3\tau'+\kappa_3')\Big], \quad \text{(a)} \\ v_{\text{forced}} &\approx \frac{Ta}{27\mu}\left(\frac{a}{r}\right)\cos 2\theta\cos\phi\Big[\eta_4'\tau'\exp\{-\zeta\tau'\}\Big], \quad \text{(b)} \\ v_{\text{complementary}} &\approx \frac{Ta}{27\mu}\left(\frac{a}{r}\right)\cos 2\theta\cos\phi\Big[\eta_5'\exp\{-\zeta\tau'\}\Big], \quad \text{(c)} \end{aligned}\right\} \tag{42}$$

$$\left.\begin{aligned} w_{\text{free}} &\approx \frac{Ta}{27\mu}\left(\frac{a}{r}\right)\cos\theta\sin\phi\Big[\eta_1'\exp\{-\beta_1\tau'\}\sin(\alpha_1\tau'+\kappa_1') \\ &\qquad +\eta_2'\exp\{-\beta_2\tau'\}\sin(\alpha_2\tau'+\kappa_2') \\ &\qquad +\eta_3'\exp\{-\beta_3\tau'\}\sin(\alpha_3\tau'+\kappa_3')\Big], \quad \text{(a)} \\ w_{\text{forced}} &\approx \frac{Ta}{27\mu}\left(\frac{a}{r}\right)\cos\theta\sin\phi\Big[\eta_4'\tau'\exp\{-\zeta\tau'\}\Big], \quad \text{(b)} \\ w_{\text{complementary}} &\approx \frac{Ta}{27\mu}\left(\frac{a}{r}\right)\cos\theta\sin\phi\Big[\eta_5'\exp\{-\zeta\tau'\}\Big], \quad \text{(c)} \end{aligned}\right\} \tag{43}$$

in which τ, τ', ζ, α_1, α_2, α_3, β_1, β_2, β_3 have the same values as in Art. 3, which are obviously independent of the time-variations in the applied pressure. $\eta_1\sim\eta_5$, $\eta_1'\sim\eta_5'$, $\kappa_1\sim\kappa_3$, $\kappa_1'\sim\kappa_3'$ are also certain functions of the rapidity of the applied shearing stress, being calculated numerically for various values of $a/(t_m v)$ as shown in Tables VIII, IX.

As in Arts. 2, 3, the longitudinal wave u_1 expressed by (38) and the transversal waves v_3, w_3 expressed by (39), (40) are respectively

Table VIII.

$\zeta(=a/(t_m v))$	η_1	η_2	η_3	η_4	η_5	κ_1	κ_2	κ_3
0·1	0·1226	−0·0642	0·1728	−0·0167	0·1808	0·046	0·214	−1·552
0·4	0·6420	−0·2726	0·9358	−0·2907	0·5933	0·167	0·437	−0·674
1·0	3·018	−0·7382	1·3166	−0·3647	−2·092	0·550	0·922	0·995
1·5	8·192	−1·0684	−0·8900	1·882	−7·297	1·142	1·331	−1·514
2·0	−19·552	1·3322	−0·6376	10·730	−14·698	−0·942	−1·3565	−1·223
3·0	−11·650	1·3364	−0·3784	13·259	9·809	−0·9025	−0·823	−0·929
5·0	3·190	1·0020	−0·2024	5·821	3·079	−1·30	−0·14	−0·72
8·0	1·3082	0·6354	−0·1204	2·803	0·8639	−1·018	0·285	−0·638
11·0	0·7990	0·4507	−0·0828	1·789	0·3835	−0·916	0·475	−0·544
15·0	0·5218	0·3208	−0·0568	1·191	0·1803	−0·818	0·595	−0·365

Table IX.

$\zeta(=a/(t_m v))$	η_1'	η_2'	η_3'	η_4'	η_5'	κ_6'	κ_2'	κ_3'
0·1	−0·066	0·0584	−1·2334	−0·0936	1·087	−0·0728	−0·538	1·037
0·4	−0·3488	0·2512	6·668	−2·116	6·373	0·0519	−0·313	−1·2276
1·0	−1·632	0·6780	9·388	−8·364	−3·438	0·431	0·170	0·441
1·5	−4 424	0·9738	6·366	−10·206	−2·349	1·024	0·580	1·0746
2·0	12·840	1·1294	4·452	−16·684	5·103	−0·956	1·109	1·381
3·0	6·284	1·2162	−2·684	−16·712	−8·332	0·784	1·566	−1·481
5·0	−1·622	−0·9130	−1·4524	−12·202	−3·807	−1·418	−0·892	−1·280
8·0	−0·706	−0·5784	−0·8524	−9·812	−1·686	−1·139	−0·464	−1·176
15·0	−0·2798	−0·2920	−0·429	−8·224	−0·659	−1·040	−0·130	−1·091

composed of three kinds of waves; [1] the forced waves expressed by (41)b, (42)b, (43)b, [2] the free waves given by (41)a, (42)a, (43)a, and [3] the complementary waves expressed by (41)c, (42)c, (43)c. The vibrations of particles due to the free waves (41)a, (42)a, (43)a, which are of damped waves, are the resultants obtained by superposing three kinds of damped oscillations with their respective damping ratios $e^{\pi\beta_1/\alpha_1}$, $e^{\pi\beta_2/\alpha_2}$, $e^{\pi\beta_3/\alpha_3}$, and also with the respective free periods $2\pi\frac{a}{\alpha_1 v}$, $2\pi\frac{a}{\alpha_3 v}$, $2\pi\frac{a}{\alpha_3 v}$.

In order to find the nature of the oscillatory vibrations of the particles that lie some distance away from the cavity due to waves (38)∼(40), we obtained Figs. 33∼41 for various values of $a/(t_m v)$. The units of the vertical scales in Fig. 33∼41 are taken as $\frac{Ta}{27\mu}\left(\frac{a}{r}\right)$.

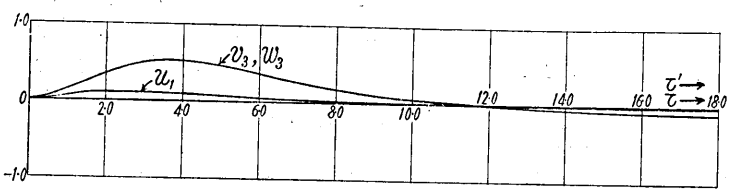

Fig. 33. $\frac{a}{t_m v}=0{\cdot}1$.

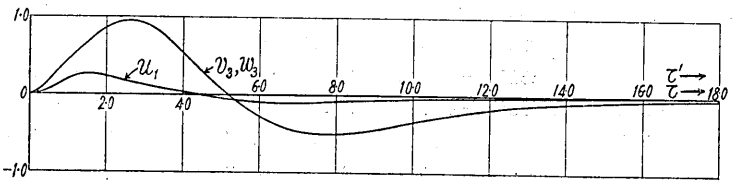

Fig. 34. $\frac{a}{t_m v}=0{\cdot}4$.

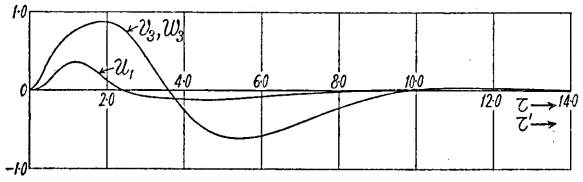

Fig. 35. $\frac{a}{t_m v} = 1{\cdot}0.$

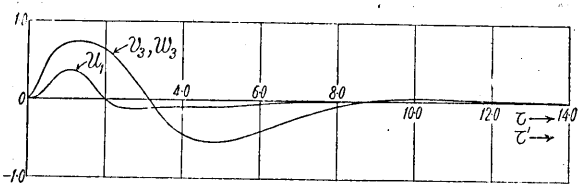

Fig. 36. $\frac{a}{t_m v} = 1{\cdot}5.$

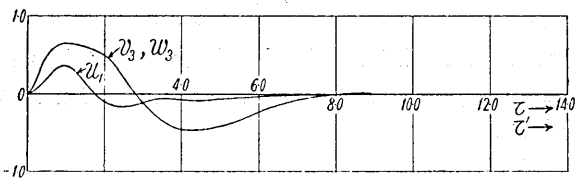

Fig. 37. $\frac{a}{t_m v} = 2{\cdot}0.$

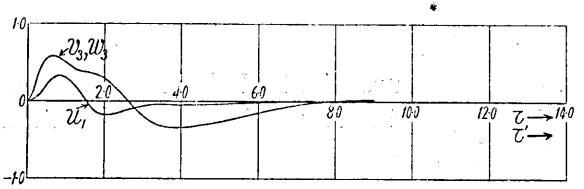

Fig. 38. $\frac{a}{t_m v} = 1{\cdot}00.$

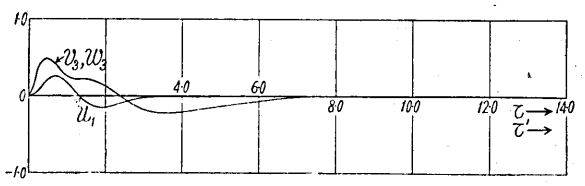

Fig. 39. $\frac{a}{t_m v} = 5{\cdot}0.$

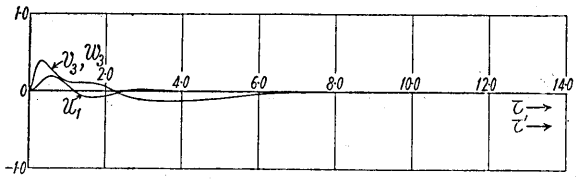

Fig. 40. $\frac{a}{t_m v} = 8{\cdot}0.$

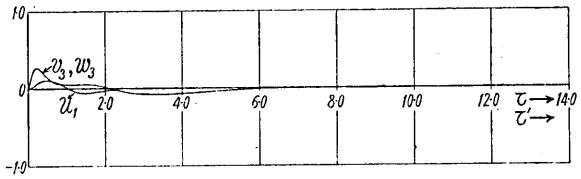

Fig. 41. $\frac{a}{t_m v} = 15{\cdot}0.$

$\sin 2\theta \cos\phi$, $\frac{Ta}{27\mu}\left(\frac{a}{r}\right) \cos 2\theta \cos\phi$, and $\frac{Ta}{27\mu}\left(\frac{a}{r}\right) \cos\theta \sin\phi$ for u_1, v_3, and w_3 respectively. Figs. 33~41 show that when shearing force of the shock type are applied to the inner surface of a spherical cavity, the particles that are some distance away from the cavity assume the character of damped oscillations due to the longitudinal and transversal waves leaving the cavity. The curves U_1, V_3, W_3 in Fig. 42, which are obtained from Figs. 33~41, show the respective vibration-amplitudes of particles in their initial motions due to the longitudinal and transversal waves. The abscissa of Fig. 42 shows the value of the rapidity of the shearing stresses applied to the cavity. As in Art. 3, we can also see from Fig. 42 that the maximum vibration-amplitudes of the particles in their initial motions due to the transversal waves are generally larger than those due to the longitudinal waves, their resonance-

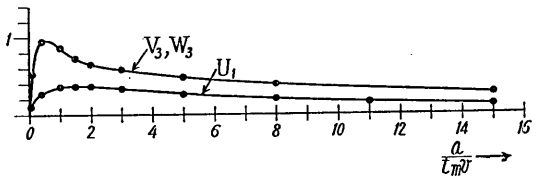

Fig. 42.

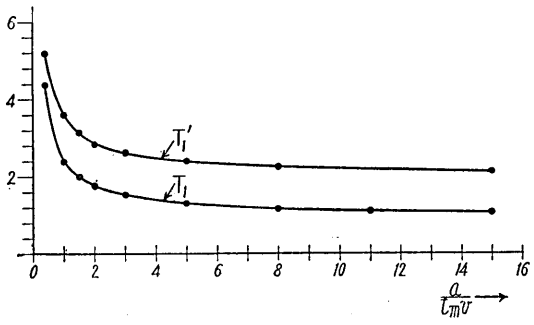

Fig. 43.

like characters being also seen from these two curves. The curves T_1, T_1' in Fig. 43 show the respective durations of time from the beginning of the vibration to the time when the displacement of the particles due to both longitudinal and transversal waves first becomes nil, and the curves T_2 and T_2' in Fig. 44 correspond to the durations of time from the beginning of the vibrations to the time when the displacement of the same particles due to the same respective waves becomes nil for the second time. Figs. 43, 44, in which the respective abscissae show the rapididy with which the shearing force was applied to tne cavity, are derived from Figs. 33~41. From Figs. 43, 44, we get an idea again of the nature of the apparent vibration-periods of the particles as in Figs. 30, 31 in Art. 3.

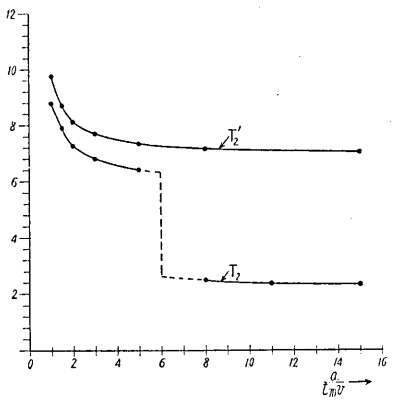

Fig. 44.

5. We may be able to study by the same method as in Arts. 3, 4, the wave-phenomena in cases where the normal and the shear components of stresses on the inner surface of a spherical cavity of radius a have space-distributions expressed by Zonal-harmonics of the second degree, such as

$$\widehat{rr}_{r=a} = P\frac{t}{t_m}\exp\{1-t/t_m\}\,P_2(\cos\theta), \quad \widehat{r\theta}_{r=a} = 0, \tag{44}$$

or

$$\widehat{rr}_{r=a} = 0, \quad \widehat{r\theta}_{r=a} = T\frac{t}{t_m}\exp\{1-t/t_m\}\,\frac{\partial P_2(\cos\theta)}{\partial\theta}, \tag{45}$$

although our detailed discussions of them are reserved for another occasion.[20]

The writers express their thanks to Professor Katsutada Sezawa for his encouragement and valuable advices.

Summary and Conclusion.

Assuming a spherical cavity in an elastic earth, we studied the

20) A paper on the mathematical results for the case in which the boundary conditions are expressed by (44) was read at the 131st Local Meeting of the Earthq. Res. Inst., (Nov. 16, 1397).

vibrational motions of particles, lying some distance away from the cavity, caused by elastic waves propagated from it for the case in which the tractions that are applied to its inner surface are of the shock type. The elastic waves due to tractions of shock type are usually longitudinal and transversal bodily waves, both of which are composed of three kinds of waves; [1] FORCED WAVES, [2] FREE WAVES, and [3] COMPLEMENTARY WAVES. The forced waves have the same time-variation as when tractions are applied to the cavity, the free waves being damped simple-harmonic time-variations. The periods and the damping ratios of the free waves are independent of the manner of the time-variation in the traction applied to the cavity, but depend upon both the elasticity of the medium and the dimension of the cavity, and also upon the mode of the intensity-distributions of the applied traction on the inner surface of the cavity. The complementary waves have time-variations of an aperiodic decaying character, like $exp\{-\alpha\tau\}$. The space-distributions of these three kinds of waves are determined by the distributions of the tractions applied to the inner surface of the cavity, and their amplitudes at any point in the medium are certain functions of the rapidity of the applied tractions.

The particles that are some distance away from the cavity, are usually damped vibrations as the result of longitudinal and transversal waves that issue from the cavity, both being the resultants obtained by superposing these free, forced, and complementary waves. Now the respective amplitudes of the co-latitudinal and azimuthal components of displacements of the propagated longitudinal wave are less than the radial component of displacement of that wave when the distance from the center of the cavity becomes very large, and those of the radial displacement due to the propagated transversal wave are less than those of the co-latitudinal and azimuthal components of displacement due to the same wave when the distance from the cavity is very great. These small quantities of displacements may therefore be disregarded in studying the wave-motions of particles that are some distance away from the cavity; in other words, the longitudinal waves that emerge from the cavity excite only the radial vibrations of the particles that are some distance away from the cavity, while the transversal waves excite only the co-latitudinal and azimuthal vibrations of the same particles.

When the distance from the center of the cavity is very great, the apparent period of the longitudinal wave in a state of initial motion is usually shorter than that of the transversal wave, the two periods being certain functions of the rapidity of the stress applied to the cavity, although the difference between them becomes nearly constant,

notwithstanding the rapidity of the applied stress when it exceeds a certain value. The more rapid the applied stress on the cavity, the shorter the two apparent periods, which, however, do not vary so much as the period of the forced wave. The reason that the relation between the apparent periods and the rapidity with which the stress is applied is not so simple as in the case of the forced wave, is the existence of both the free and complementary waves in addition to the forced wave.

The amplitudes of vibration of the particles that are some distance away from the cavity, which vibrations are due to the longitudinal and transversal waves issuing from the cavity, are also certain functions of the rapidity of the applied stress, showing a spectrum-like character in its variations. Generally speaking, for a certain range of the rapidity of the applied stress, the amplitudes due to longitudinal waves are smaller than those due to transversal waves. When the rapidity becomes very large, the amplitudes due to the transversal wave may become smaller than those due to the longitudinal wave.

The mathematical results shown in this paper have not been verified with seismometrical data on an actual earthquake, the mechanism of occurrence of certain deep-earthquake being merely discussed by using both the experimental results obtained by H. Honda, as already mentioned, and the present theoretical results obtained by us, to which have added a brief outline of our ideas on earthquake origin.

The present paper concerns only wave-phenomena that occur at places some distance away from the assumed cavity, reserving for a future occasion our studies of phenomena that occur near the cavity for the case when the inner surface of the cavity is subjected to tractions of shock-type as assumed in Arts. 3, 4.

27. 彈性地殻內にある球狀震源より出る地震波

地震研究所 西村源六郎
高山威雄

著者の一人西村は以前に彈性地殻內に球狀空窩が存在してゐると假定し，その空窩內面に衝撃型の壓力が作用した時に發生する地震波を研究して置いた.[1] 本論文はその延長と見るべきものであるが，計算結果を多數の圖面に示めし，地震波生成に關して相當面白いと思はれる結果を得る事が出來た. 卽ち振動性 P 波 S 波の生成，それ等の初動の週期，振幅，或は波長に關して彈性波動學論的に興味あるのみならず，實驗上或は驗震學的に得た事實を說明するに大切な理論的結果を得た.

尙これは實驗的に證明されるかも知れないが，震源より出る地震波は，P 波 S 波何れにせよこれを解析すれば，强制波，自由波及び初期波の三種より成立つてゐる事が解かつたのであるがこれも研究結果の一つである. 若し實驗的にこの强制波を取出す事が出來れば，震源での力の變り方が明かにされ，發震機構の研究を一步進める事が出來るのである.

---

1) 西村源六郎，地震研究所彙報 **15** (昭和 12 年)，3 號.